TOGA COARE: The Coupled Ocean–Atmosphere Response Experiment

Peter J. Webster*
and Roger Lukas+

Abstract

Despite significant progress in the Tropical Ocean–Global Atmosphere (TOGA) program, a number of major hurdles remain before the primary objective, prediction of the variability of the coupled ocean–atmosphere system on time scales of months to years, can be achieved. Foremost among these hurdles is understanding the physics that maintains and perturbs the western Pacific warm pool, the region of the warmest sea surface temperature in the open oceans, which coexists with the largest annual precipitation and latent heat release in the atmosphere. Even though it is believed that the warm pool is a "center of action" for the El Niño–Southern Oscillation (ENSO) phenomena in the ocean and the atmosphere, successful simulation of the warm pool has remained an elusive goal.

To gain a clear understanding of global climate change, the ENSO phenomenon, and the intraseasonal variability of the coupled atmosphere–ocean system, it is clear that a better specification of the coupling of the ocean and the atmosphere is required. An observational and modeling program, the TOGA Coupled Ocean–Atmosphere Response Experiment (TOGA COARE), has been designed to work toward this goal.

The scientific goals of COARE are to describe and understand:

1) the principal processes responsible for the coupling of the ocean and the atmosphere in the western Pacific warm-pool system;

2) the principal atmospheric processes that organize convection in the warm-pool region;

3) the oceanic response to combined buoyancy and wind-stress forcing in the western Pacific warm-pool region; and

4) the multiple-scale interactions that extend the oceanic and atmospheric influence of the western Pacific warm-pool system to other regions and vice versa.

To carry out the goals of TOGA COARE, three components of a major field experiment have been defined: interface, atmospheric, and oceanographic. An intensive observation period (IOP), embedded in a period of enhanced meteorological and oceanographic monitoring, will occur from November 1992 through February 1993 in the western Pacific region bordered by 10°N, 10°S, 140°E, and the date line. The experimental design calls for a complex set of oceanographic and meteorological observations from a variety of platforms that will carry out remote and in situ measurements. The focus of the observational effort will be in an intensive flux array (IFA) centered at 2°S and 156°E. The resulting high-quality dataset is required for the calculation of the interfacial fluxes of heat, momentum, and moisture, and to provide ground truth for a wide range of remotely sensed variables for the calibration of satellite-derived algorithms. The ultimate objective of the COARE dataset is to improve air–sea interaction and boundary-layer parameterizations in models of the ocean and the atmosphere, and to validate coupled models.

*Program in Atmospheric and Oceanic Sciences, University of Colorado, Boulder, Colorado
+Department of Oceanography, Honolulu, University of Hawaii

1. Introduction

During the last decade there has been an unprecedented interest in the dynamic interactions of the ocean and the atmosphere. Vast amounts of data have been collected, and coupled ocean–atmosphere models have been developed. The purpose of this activity has been to establish the physical basis for the variability of climate on interannual time scales and, if possible, forecast the variability. With these goals in mind, the international community launched the Tropical Ocean–Global Atmosphere (TOGA) program, which allowed considerable resources to be brought to bear on the problem.

TOGA is a major component of the World Climate Research Programme (WCRP 1985) aimed specifically at the prediction of climate phenomena on time scales of months to years. The philosophy upon which TOGA is based purposefully emphasizes the tropical oceans and their relationship to the global atmosphere. Underlying TOGA is the premise that the dynamic adjustment of the ocean in the tropics is far more rapid than at higher latitudes and, therefore, more closely in tune with the atmosphere. The specific goals and scientific objectives of TOGA are (WCRP 1985):

- to gain a description of the tropical oceans and the global atmosphere as a time-dependent system in order to determine the extent to which the system is predictable on time scales of months to years and to understand the mechanisms and processes underlying its predictability;
- to study the feasibility of modeling the coupled ocean–atmosphere system for the purpose of predicting its variations on time scales of months to years; and
- to provide the scientific background for designing an observing and data-transmission system for operational prediction, if this capability is demonstrated, by coupled ocean–atmosphere models.

In order to achieve the TOGA goals, a strategy of long-term monitoring of the upper ocean and the atmosphere, intensive and very specific process-oriented studies, and modeling has been developed (WCRP 1985). The plans have been enacted through a series of national, multinational, and international efforts (e.g., National Academy of Sciences 1986; WCRP 1986).

The TOGA program has passed the midway point of the ten-year period of intensified monitoring and modeling activities. In the second half of the TOGA observing period, the thermodynamical structure of the upper regions of the tropical oceans has begun to be monitored on a regular basis with a scale, frequency, and intensity similar to that which has long been considered normal for the atmosphere. Process studies have been conducted focusing on specific aspects of the dynamical structure of the tropical ocean waveguide, turbulent mixing of the upper ocean, and the distribution of salinity. These studies have concentrated on understanding the processes responsible for the equatorial cold tongue, its relation to eastern-boundary circulation, and the relative importance of local and remote forcing on the eastern and central Pacific Ocean. Long-term monitoring of the structure of the tropical ocean has been achieved by an XBT (expendable bathythermograph) program and by the TOGA Tropical Atmosphere–Ocean (TAO II) buoy array, which spans the entire Pacific basin between 8°N and 8°S, the TOGA/World Ocean Circulation Experiment (WOCE) Pan-Pacific drifting-buoy program, and the TOGA sea level network. In addition, the low-latitude meteorological sounding and surface observation network has been augmented and the FGGE [First Global Atmospheric Research Program (GARP) Global Experiment] surface drifting-buoy program in the Southern Hemisphere has been continued.

A major achievement in TOGA has been the determination of the relative importance of the Atlantic, Indian, and Pacific ocean basins in producing the interannual El Niño–Southern Oscillation (ENSO) signal.

A major achievement in TOGA has been the determination of the relative importance of the Atlantic, Indian, and Pacific ocean basins in producing the interannual El Niño–Southern Oscillation (ENSO) signal. The tropical Pacific Ocean has emerged as the predominant basin in ENSO. The relationship of the Pacific Ocean to other tropical regions and to the global atmosphere is as follows: The Pacific Ocean undergoes strong interannual variability with a time scale of three to five years. It has been argued that this variability appears to be an internal dynamical mode of the coupled ocean–atmosphere system of the tropical Pacific basin (see Philander 1990 for review). The variation is transmitted very rapidly eastward along the equatorial ocean waveguide. The resulting variation of the sea surface temperature (SST) (Fig. 1a) drives an atmospheric response that encompasses the entire tropics (Fig. 1b). In turn, this response is translated to remote, planetary-scale, wind-stress forcing functions on the surfaces of the other two basins. Thus, following ENSO variations in the Pacific structure, the Atlantic and Indian oceans are affected by anomalous wind forcing originating in the Pacific. This scheme emphasizes the importance of the Pacific Ocean in general, and the warm-water regions in particular. It does not mean that variations in the other oceans are less important, as it is obvious that they invoke changes in local tropical circulations such as in the Brazilian region (Moura and Shukla 1983) and the south Asian region (e.g., Shukla and Paolino 1983; Rasmusson and Carpenter 1983). Rather, it allows variations in the Atlantic and Indian oceans to be placed in a sequential perspective on ENSO time scales.

Theoretical constructions have attempted to explain the variability of the Pacific Ocean basin. In general, these theories cluster around the instability of the coupled ocean–atmosphere system or its quasi-cyclic variation (Philander 1990). Both families of theories depend on the character and structure of the coupled system. The instability theory describes the growth of unstable modes of the basic state of the coupled system, and the quasi-cyclic theory depends on successive reflections of neutral, equatorially trapped ocean models from the boundaries of the Pacific basin within the basic state of the joint system (Graham and White 1988). These two theories are probably not mutually exclusive as it is possible that both the instability and cyclic processes work together to produce the diverse spatial and temporal scales of ENSO.

Modeling and assimilation efforts within TOGA have led to the first quasi-operational ocean–atmosphere prediction model running in near-real time, initialized with data collected from the TOGA monitoring network (see Cane 1990). Experimental efforts to couple ocean and atmospheric models in order to synthesize the total system have been vigorous. Phenomenological models have produced a clearer view of how the tropical atmosphere and ocean combine to produce a

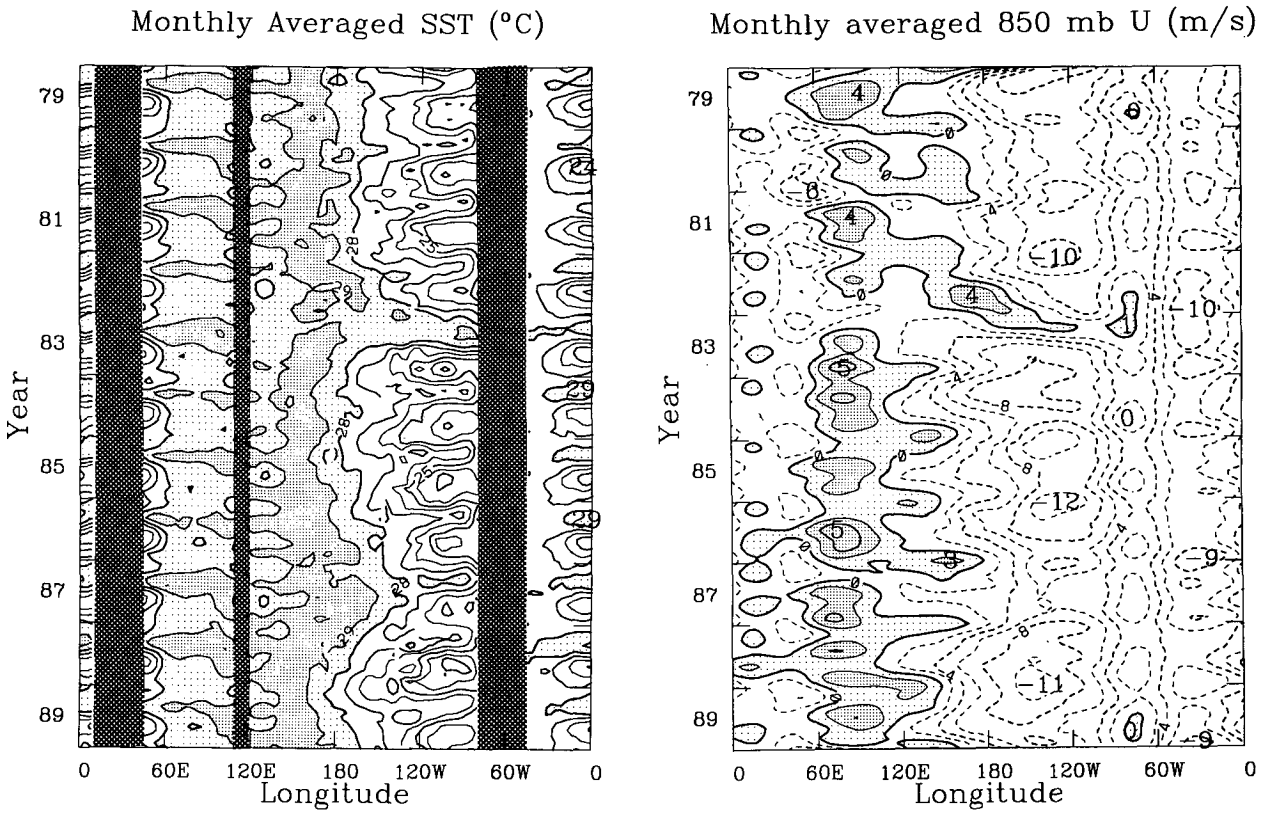

FIG. 1. (a)Time–longitude distribution averaged between 4°N and 4°S of the mean monthly sea surface temperature (SST; °C) between January 1979 and December 1989. The shaded regions denote (left to right) the land masses of Africa, Indonesia, and South America. Light and heavy shading regions depict SSTs in excess of 28°and 29°C, respectively. Note the two major "warm events" (i.e., El Niño) in 1982–83 and 1986–87. In contrast, 1988 was a "cool" event (La Niña) where the warm waters contract to the western Pacific Ocean. Data from the NOAA Comprehensive Ocean–Atmosphere Data Set (COADS).

robust interannual signal. Thus, there has been considerable progress toward the primary goals of TOGA through these observational and modeling efforts. A critical review of the first half of the TOGA program is given by the National Research Council (NRC 1990).

Despite substantial progress gained thus far during the TOGA program, there is still considerable doubt regarding the elementary physical processes that maintain the mean and transient states of the warm-water regions of the eastern Indian and western Pacific oceans. These doubts restrict our ability to model adequately the coupled atmosphere–ocean system and form obstructions to improvements in forecasting ability. Some of the concerns are:

- Diagnostic studies find balancing the surface energy budget of the Pacific warm pool to be an elusive goal. Some estimates possess an unexplained residual in the surface energy balance of order 60–80 W m^{-2} (cf. Godfrey and Lindstrom 1988).
- The simulated warm-pool surface temperatures of stand-alone ocean models are often too warm when the model is forced with either heat fluxes derived from climatological data or from those derived by atmospheric models. Realistic model simulations have been achieved only using carefully tuned heat fluxes at the ocean surface together with an assumed climatological cloud cover (Gent 1991).
- One of the weaker links in both simple coupled models and coupled GCMs is the nature of interactions in the western tropical Pacific. In coupled models that simulate ENSO, the westerly wind anomalies in the model western Pacific are weaker than observed in nature (Hirst 1988; Cane 1990). It is not clear whether this is due to deficiencies in the model physics or to exclusion of western Pacific atmospheric interactions with the tropical atmosphere over other ocean basins and/or with the extratropical atmosphere (e.g., Gutzler and Harrison 1987; Meehl 1987).

It is clear from the above that a careful set of measurements in the warm-pool region of the Pacific Ocean is needed. It is only through such efforts that significant model improvement for both diagnostic and

forecasting purposes can be realized. In the next section, a broad description of the phenomenology of the atmosphere and the ocean of the tropical warm-pool regions is given. Section 3 outlines the scientific objectives of the TOGA Coupled Ocean–Atmosphere Response Experiment (COARE), a program designed to address the concerns listed above, and basic strategies to be employed. The scientific objectives of the individual elements of COARE are listed in section 4. The overall experimental design of COARE with particular emphasis on the intensive observation phase (IOP) is presented in section 5.

2. The scientific basis for TOGA COARE

The largest region of warm water lies in the western Pacific and eastern Indian oceans. Figure 2a shows the long-term average distribution of SST for the boreal winter. The 28°C isotherm is shown as the heavy contour. The significance of the warm pools to the general circulation of the atmosphere can be seen from Fig. 2b, which shows the smoothed total diabatic heating in the atmospheric column between 750 and 50 mb calculated from the European Centre for Medium-Range Weather Forecasts (ECMWF) initialized data (Hoskins et al. 1989). The field represents contributions from latent, radiative, and sensible heating from a broad range of scales of phenomena. The clear correspondence of the warm pools with the maxima of the total heating indicates the role of the warm pool in setting atmospheric global-heating gradients and, by extension, the importance of warm-pool phenomena in the general circulation of the atmosphere.

A variety of phenomena occur in both the ocean and the atmosphere within the tropical warm pools and the warm pool in the western Pacific Ocean in particular. One special characteristic appears to link the phenomena within the warm pool: In the ocean and the atmosphere individually, and jointly within the coupled system, the phenomena interact strongly over broad time and space scales.

a. Structure of the atmosphere over the warm pool

1) Global context of the warm pool

Air–sea interaction in the western tropical Pacific is dominated by the large-scale atmospheric convergence associated with the ascending branch of the Walker circulation, with the major tropical ascent occurring over the Pacific–Indian ocean warm pool (e.g., Webster 1983). The convergence of air and moisture from the Pacific and Indian oceans leads to vigorous convection and heavy precipitation and the release of latent heat in the atmosphere, which drives the Walker circulation (Cornejo-Garrido and Stone 1977; Hartmann et al. 1984). Figure 3 shows an estimate of the annual average precipitation over the Pacific Ocean by Taylor (1973). Precipitation appears to be widespread with extrema of over 5 m yr^{-1} and an overall average in excess of 3 m yr^{-1} over the warm pool.

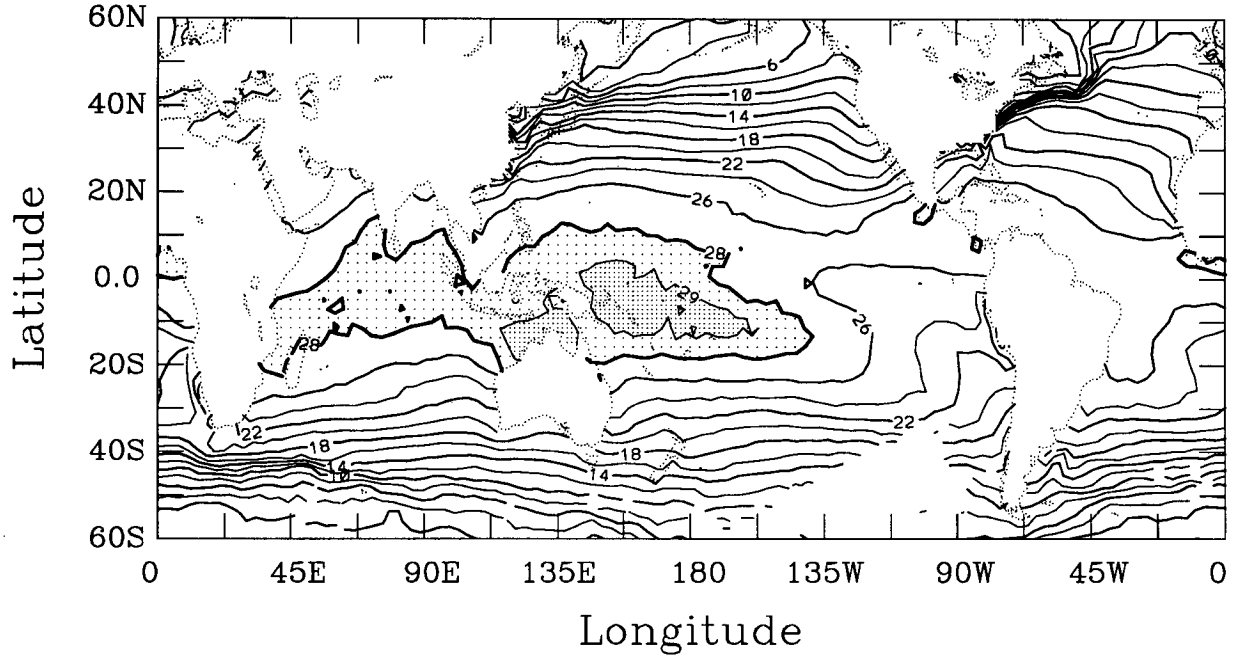

Fig. 2. (a) The long-term mean (1959–1989) boreal winter (December–February) SST (°C) distribution. Lightly and heavily shaded regions denote temperatures in excess of 28° and 29°C, respectively. Blank areas in the Southern Hemisphere indicate insufficient data. Data from COADS.

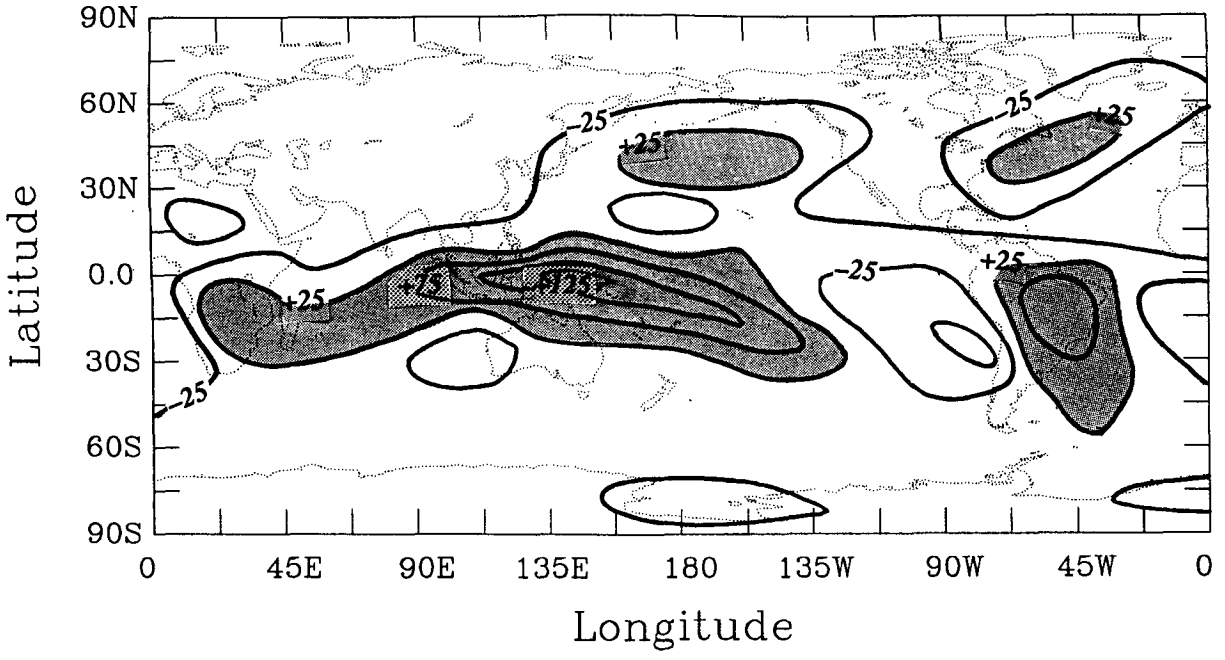

FIG. 2 (continued). (b) The smoothed total diabatic heating for the boreal winter (December–February) in an atmospheric column betweeen 700 and 50 mb (from Hoskins, et al. 1989). Units Wm^{-2}. Field was calculated as a residual from the time-averaged thermodynamic equation using ECMWF data for the six-year period December 1983–February 1989. Contour interval is 50 Wm^{-2} and shaded areas show regions in excess of 25 W m^{-2}. Central values exceed 200 W m^{-2} which is equivalent to a net heating rate of the column of 2.7 K day^{-1}. Note the correspondence of the major diabatic heating maximum with the tropical Indian and Pacific ocean warm pools.

The SST maximum of the warm pool is probably associated with the convergence of the oceanic circulation in the western tropical Pacific and the production of a relatively deep thermocline forced by the general atmospheric convergence of the Walker Circulation in the area. Thus, the warm pool is the product of interaction between the ocean and the atmosphere. Along with the normally deep thermocline, the combination of generally light winds, which are not energetic enough to cause deep mixing in the ocean, and heavy precipitation, which provides a fresh, stable ocean surface layer, tends to minimize surface cooling of the warm pool. In the near-equatorial region north of Papua New Guinea, for example, the long-term monthly mean wind speeds are always less than 3 m s^{-1}, and are usually close to 1 m s^{-1} (Sadler et al. 1987). The annual average wind stress for the region 4°N–4°S, 140°–160°E is given by Wyrtki and Meyers (1976) to be 2.5×10^{-3} N m^{-2}, roughly equivalent to a mean wind speed of 1.2 m s^{-1}. Such conditions prevail in regions with precipitation in excess of 4 m yr^{-1}.

Within these low mean wind-speed conditions, an approximately one-dimensional radiative–convective equilibrium (cf. Betts and Ridgeway 1988) seems to hold in which the strong coupling between cumulonimbus heating and radiative cooling provides a negative feedback that stabilizes the system with near-zero net heat flux on average. This feedback is not able to damp out the diurnal cycle, however, and the waxing and waning of convection in response to diurnal radiative heating of the sea surface can be observed (Lukas 1991).

Strong cloud variability over the warm pool associated with the convective activity translates into large variations in the solar radiational flux at the ocean surface (Ramanathan 1987; Webster 1991). Variations in solar flux translate into variations in the total radiative flux, because the high moisture content of the boundary layer above the warm pool renders the atmosphere optically black, which mitigates the effects of cloud on the downwelling longwave radiation. Thus, decreases in solar radiation are not compensated by enhanced IR from the cloud base to the degree that occurs at higher latitudes where the boundary layer is drier. Ramanathan and Collins (1991) have speculated that the rapidly diminished solar flux, which accompanies convective growth in the warm pool, acts as a natural regulator of the SST. While the hypothesis has yet to be tested with field data, it is clear that the magnitude of the variability of net radiation at the surface of the warm pool is as large as anywhere on the globe and must, therefore, be understood.

The importance of upper-ocean mixing processes in this balance was elucidated by Sarachik (1978); in the mean, the atmosphere is affected only by the ability of the ocean to provide moisture for latent

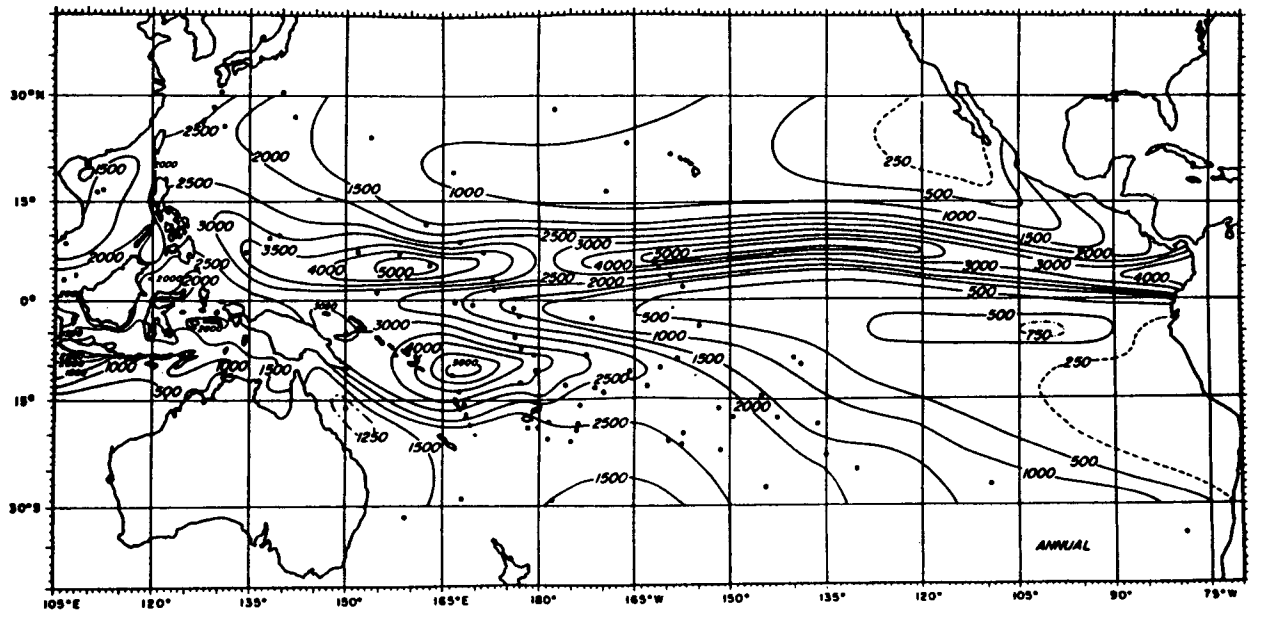

FIG. 3. Distribution of the mean annual precipitation (mm) as calculated from long-term time series of tropical island precipitation by Taylor (1973). To the west of the date line, the areal average precipitation exceeds 3 m year^{-1} with extrema of 5 m year^{-1} to the north and south of the equator.

heating, while variations around this mean state depend on the detailed thermodynamics of the ocean surface mixed layer. Recently, the importance of the complete hydrological cycle in this coupling has also become apparent, both in observations (Lukas 1990a,b) and in simple models (Chu and Garwood 1991). The one-dimensional models must specify the large-scale background moisture convergence in the atmosphere, and the background upwelling or downwelling in the ocean. These parameters influence the magnitude and even the sign of the feedbacks locally between air and sea but are themselves set by the large-scale oceanic and atmospheric circulation.

The western Pacific Ocean is a region of net freshwater input into the ocean. Estimates of rainfall and evaporation result in a net freshwater flux of 1 to 2 m yr^{-1}. This mass and buoyancy flux significantly affects the dynamics and thermodynamics of the mixed layer of the western Pacific warm pool (e.g., Ostapoff et al. 1973; Miller 1976). Direct thermal effects associated with precipitation may act as a negative feedback on convection (Greenhut 1978).

Much of the moisture that is precipitated in the convective cell is evaporated locally from the sea surface in the undisturbed environment around the convective region; however, the net 1–2 m yr^{-1} must be imported from outside the warm-pool region by large-scale circulation. It is crucial that the evaporative flux of moisture is understood because the latent heat is a major component of the surface heat budget. Also, the upper-ocean salinity budget cannot be balanced without better estimates of the local evaporation and, equally crucially, the local rainfall.

2) CONVECTIVE VARIABILITY OVER THE WARM POOL

Outgoing longwave radiation (OLR) variances in the 1–5- and 40–50-day bands (Lau and Chan 1988) are shown in Fig. 4. The heavy line represents the seasonal mean 28°C isopleth (and hence the warm pool), which encloses the majority of active convection in the tropics. Lau and Chan (1986, 1988) found remarkable similarities between the dominant heating pattern associated with the 30–60-day oscillation (cf. Madden and Julian 1972) and ENSO. Both are associated with the eastward propagation of a zonally oriented dipole-like heating anomaly from the eastern Indian Ocean to the western and central equatorial Pacific Ocean. Lau and Chan used the similarity to suggest that the 30–60-day oscillation and ENSO may be associated with the same type of intrinsic modes of variability, and that the former may act as a trigger for the onset of ENSO through the excitation of unstable coupled ocean–atmosphere modes.

In the warm-pool regions of the Pacific Ocean, there are many scales and forms of convection. Figure 5 (Machado and Rossow 1992) show the frequency of cluster occurrence as a function of scale for the western Pacific (GMS and GOES-W), the eastern Pacific (GOES-E) and the Atlantic (Meteosat). The

size of the convective elements was determined by the area coverage of IR temperature < 208 K. Except for the very largest scales, there is very little difference from one ocean to the other. Machado et al. (1992) and Machado and Rossow (1992) have noted that cluster frequency decreases as the inverse square of the radius of the disturbance indicating that, in a statistical sense, the warm pools are covered by approximately the same area of convection irrespective of size. Mapes and Houze (1992) have also computed size spectra of convective elements for three boreal winters in the western Pacific and find similar results.

Observational evidence provided by Nakazawa (1988) and Lau et al. (1988) relates the 1–5- and 30–60-day convective maxima shown earlier in Fig. 4a. Figure 6a shows Nakazawa's (1988) analysis of the anomalous OLR (i.e., seasonal trend has been removed and only OLR < 210 W m^{-2} is shown) averaged between 5°S and 5°N. The pattern shows a general, slow eastward propagation of the OLR minima into the COARE region (dashed line to 180°E), where they appear to achieve maximum intensity. Collectively, the propagating bands, labeled (A...D), appear to represent the convective phase of the 30–60-day mode. Each feature appears to have about a 10-day period and an eastward-propagation speed of about 10 m s^{-1}. There is little convection in the warm-pool region before event A and after D (i.e., in May and July). When each of the events is examined closely and only the "coldest" cloud (i.e., OLR < 190 W m^{-2}) is plotted as in Fig. 6b, eastward-moving features are still present but with a higher-frequency mode superimposed, which has a retrograde phase speed of about −12 m s^{-1}. Thus, relative to the low-frequency mode, the propagation speed is westward at over 20 m s^{-1}. The complex of the eastward low-frequency envelope and westward high-frequency mode is referred to as a supercluster (cf. Nakazawa 1988; Lau et al. 1988).

The dynamic fields also show large spatial scales and temporal coherence. Figure 7 shows the 5-day average 850-mb zonal wind field averaged in the latitudinal belts 5°N–5°S and 5°–10°S. The sections show time–longitude sections from October through March in 1988-89 between 0° and 180°. The fields

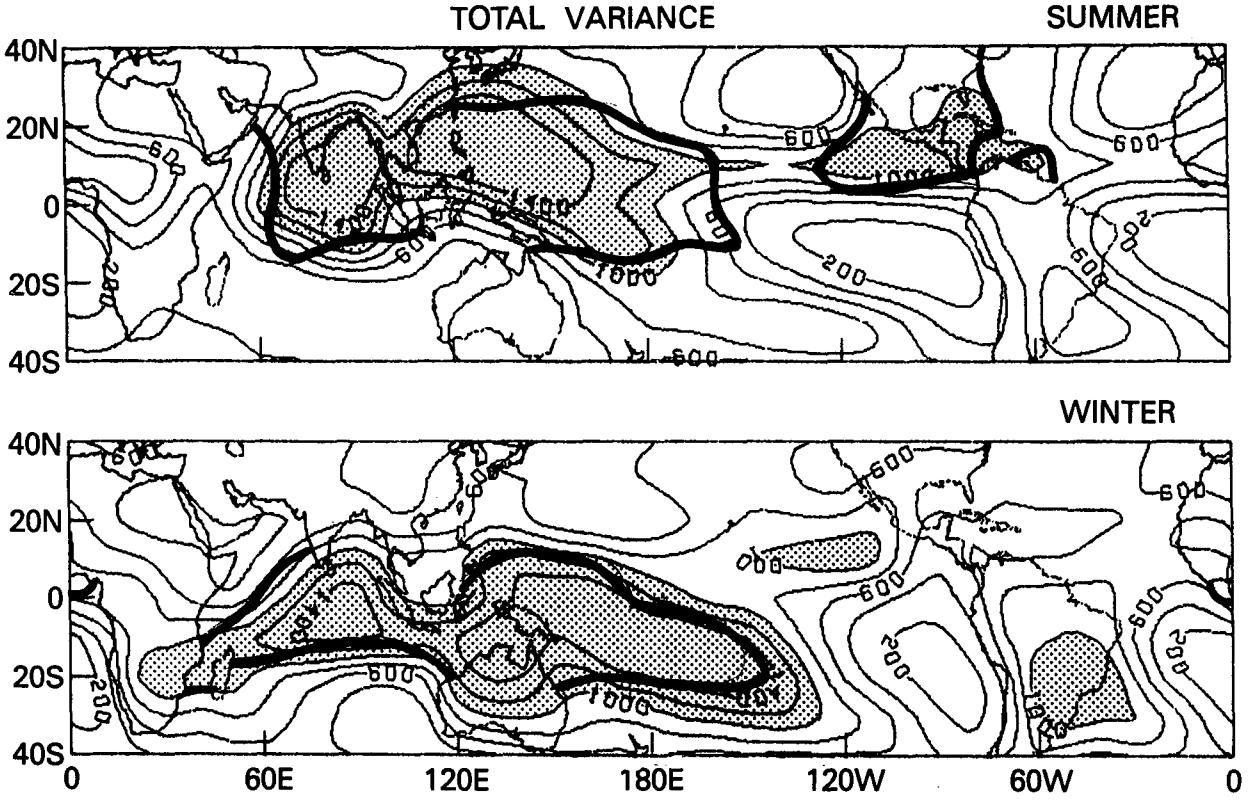

FIG. 4. The distribution of the variance of the outgoing longwave radiation (OLR: W^2 m^{-4}) from the long-term mean (June 1974–April 1986) for the boreal summer (upper panel) and winter (lower panel). Shaded area indicates variance 1000 W^2 m^{-4}. The heavy line shows the location of the 28° C SST isotherm. Variance of OLR indicates convective variability that appears to reside mainly in the tropical warm pools. Intraseasonal and synoptic components of the total variance possess essentially the same patterns. Adapted from Lau and Chan (1988).

show very long-period episodes of easterlies and westerlies with coherence lasting weeks and extending from the western Indian Ocean to the date line. These strong westerly events are referred to as "westerly wind bursts."

3) Atmospheric heating profiles

The vertical heating profile resulting from convection provides the link between the regional-scale features discussed above and the planetary-scale domain. Because some processes associated with convection (like precipitation or the transfer of momentum between the atmosphere and the ocean associated with convective gustiness) are not reversible, individual convective events contribute to the time-mean heating of the atmosphere and the mixing of the ocean. Thus, it is important to understand the convective life cycle over the warm pool.

A comparison of the vertical heating profiles compiled in a number of experiments is given in Fig. 8. A major aim during the GARP Atlantic Tropical Experiment (GATE) was to measure the convective life cycle and the resulting vertical heating profile in the tropical Atlantic Ocean and to relate those properties to the larger-scale dynamics of the tropics. Compared to earlier studies using Marshall Islands data (curves labeled Yanai et al. 1973; Reed and Recker 1971, in Fig. 8), the GATE profiles (labeled Thompson et al. 1979) were quite different. The western Pacific data show a much higher maximum heating than in the Atlantic. Furthermore, data from the Australian Monsoon Experiment (AMEX), composited from four convective events in the Gulf of Carpentaria, show very similar results to early western Pacific Ocean studies. The AMEX profile (labeled AMEX; Keenan and Carbone 1992) possesses a maximum that is at a higher level than the GATE profile. Webster (1991) speculates that the higher heating maximum is important in maintaining the dominance of convection over the warm pool compared to cooler regions.

McBride and Holland (1989) also show that there are differences between the life cycles of the Atlantic and Australian convective disturbances. Maximum heating of the GATE disturbances originated in the lower troposphere and extended to the upper troposphere through their life cycle. In similar AMEX disturbances the maximum heating started at a higher level in the troposphere and only rose slightly. Unfortunately, datasets specifically aimed at examining the life cycle of convective systems, such as those developed during GATE and AMEX, do not exist for the western Pacific Ocean. It is important to determine whether or not similarities between the mean convective heating profiles of AMEX and the early western Pacific Ocean profiles, shown in Fig. 8, extend to a similarity in life cycles as well.

4) Convective life cycle

The differences between the Atlantic and Pacific profiles may depend on the regional differences in large-scale atmospheric flow. The western Pacific region is one of the largest latent heating sources in the tropics as assessed by net OLR. The deep convective clouds provide an anchor for the largest horizontal gradient of net radiative vertical flux convergence in the tropics (Ramanathan 1987; Webster 1991). Also, a number of studies (e.g., Lindzen 1967; Hartmann et al. 1984) have suggested that atmospheric circulations are very sensitive to the fine structure of the vertical heating profile. Hartmann et al. (1984) showed that both planetary-scale tropical circulation and communication between the tropics and higher latitudes change substantially with different profiles. To improve modeling, the determination of the temporal and spatial variations of the vertical heating profile is crucial.

Figure 9 shows four typical distributions of convection encountered in the western Pa-

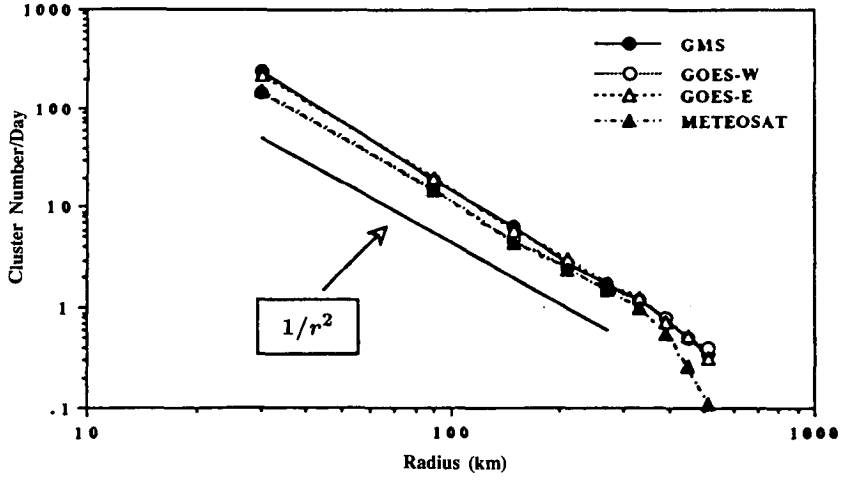

Fig. 5. The number of clusters observed per day over the tropics as a function of the cluster size during the summer and winter of 1987–88 (Machado and Rossow 1992). Scale of the disturbances are determined by the radius of cloudy regions with IR effective temperatures < 208 K. Distributions are shown for the western Pacific (GMS and GOES-W), the eastern Pacific (GOES-E), and the Atlantic (METEOSAT). The distributions tend to follow an inverse square law (solid line) with the radius of the disturbance indicating that the total area of deep cloud cover is approximately the same over the tropical oceans, irrespective of the scale of the components.

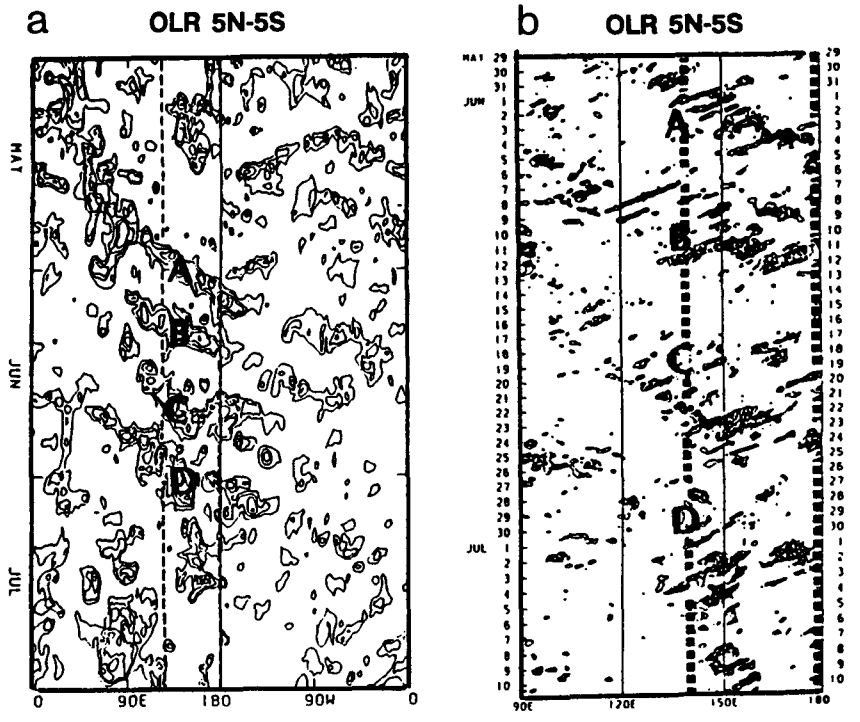

FIG. 6. Large-scale organization of convection in the tropics. (a) Time–longitude section of the OLR (W m^{-2}) with the seaonal trend removed. Contour interval is 30 W m^{-2} with a threshold of −15 W m^{-2}. The lettering (A, B, etc.) denotes the locations of eastwardly propagating "superclusters." (b) Detail of (a) emphasizing the western Pacific Ocean. Only the deepest convection (OLR <190 W m^{-2}) is shown. The superclusters now appear as eastward-moving envelopes with higher-frequency deep convective clusters propagating to the west. From Nakazawa (1988).

cific in ascending scales of organization. The vectors refer to the 850-mb ECMWF wind fields. The pictures show convection in ascending order of organization. Concentrating on the region to the south of the equator, Fig. 9a shows patterns of organized convection with scales of order 20–30 km. Larger patterns of convection appear in a northwest–southeast band but these appear to be associated with substantial convection over islands. Figure 9b shows convection of scale 100 km, which appears as distinct mesoscale disturbances. Figures 9c and 9d show disturbances with scales upward of 250 km. Figure 9c appears as a very disturbed region along the equator. In Fig. 9d the disturbances have grown into a pair of cyclonic storms, each of which later attained tropical cyclone intensity. In this latter case, note the very strong westerly winds along the equator. Cyclonic pairs are often associated with westerly wind bursts along the equator (Keen 1982).

5) ORGANIZATION AND PROPAGATION OF CONVECTION

The organization of convection is of considerable interest because it lies at the heart of heat, moisture, and momentum fluxes, which are not likely to be quantified from mean, undisturbed conditions. Ordinary tropical cumuli have short lifetimes and low convective available potential energy (CAPE), generate little kinetic energy, process relatively small quantities of condensate (none of which is from stratiform processes), and serve to lower the mean tropospheric shear through vertical mixing of momentum.

OLR observations (e.g., Nakazawa 1988; Lau et al. 1988) and the Doppler radar observations of Keenan and Carbone (1992) tend to refute the simple notion of aggregated tropical cumuli. Furthermore, a significantly higher degree of convective organization and intensity is suggested over the warm pool than was observed in GATE.

Why is organized convection so important in the tropical warm pools? Organized convection produces more condensate per unit of cloudiness as gauged by conventional measures from space. It contains a substantial component of stratiform precipitation, which markedly alters the radiative balance, latent heating aloft, and cooling at the ocean's surface. Organized mesoscale convective systems sharply increase mean tropospheric shear and thereby transport very strong momentum and dry air to the surface for periods of order 10 and areas of order 10^5 km^2. Given the low mean wind and high mean humidity over the warm pool, intermittency associated with mesoscale convective systems may dominate the quantification of interfacial and related boundary-layer fluxes. Time series of daily average winds, for example, neither reveal nor resolve these processes.

Finally, organized convective systems generally propagate with respect to larger-scale environment. The ensemble propagation of mesoscale convective systems may influence propagation of the warm pool itself because of a systematic phase displacement of the various fluxes with respect to larger-scale atmospheric/ocean forcing mechanisms.

While the organization of convection, in itself, is not of intrinsic interest to TOGA, it is believed to be a zeroth-order problem that must be quantified before

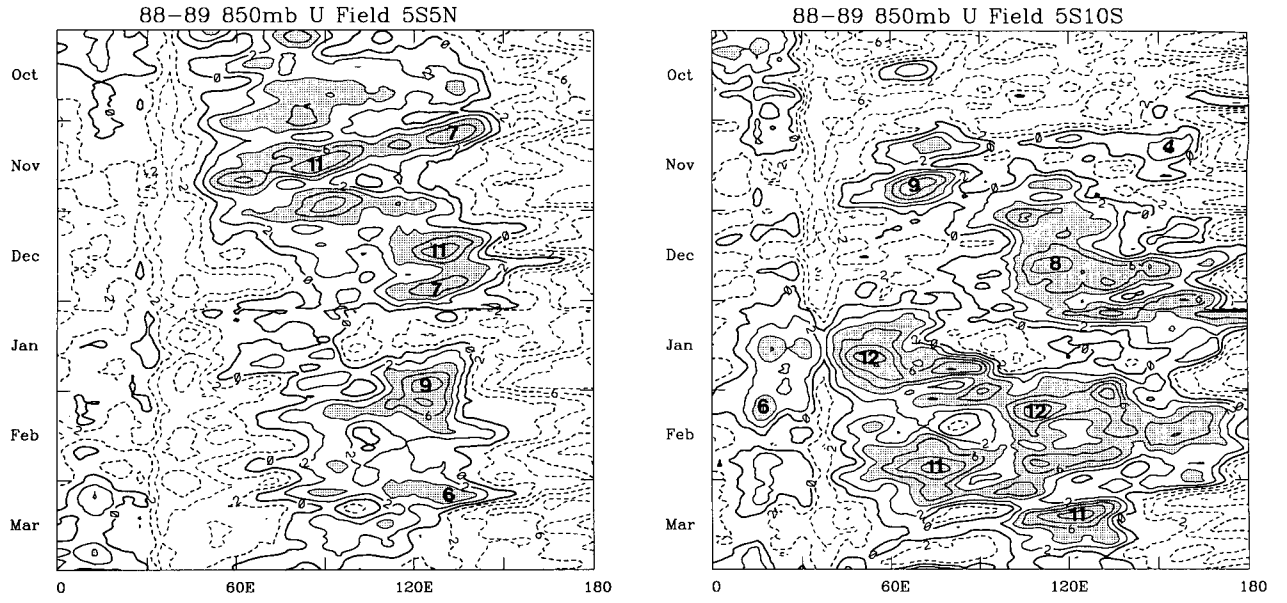

FIG. 7. (a) Time–longitude section of the 850-mb zonal wind component averaged between 5°N and 5°S from October 1988 through March 1989. A five-day running mean has been applied. The zero conour is shown as the heavy isopleth and the shading denotes westerly winds > 4 m s^{-1}. Easterlies are dashed. Note the occasional eastward excursions of the westerly winds ("westerly bursts") into the warm-pool regions. Bold figures denote the maximum 5-day average speed of the bursts. From Webster and Change (1991). (b) Same as (a) except for the latitude band 5°S–10°S.

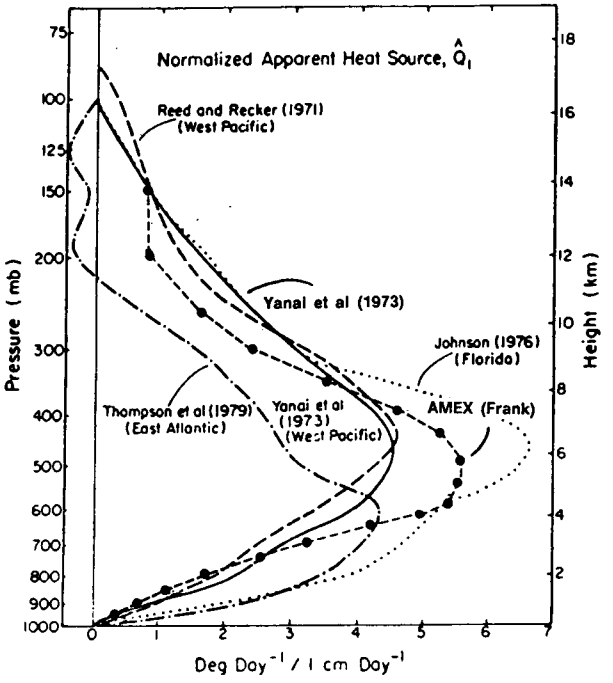

FIG. 8. A comparison of the vertical heating profiles from the GATE region in the eastern Atlantic Ocean (dash-dot: Thompson et al. 1979), the western Pacific Ocean (dashed: Reed and Recher 1971; and solid: Yanai et al. 1973), Florida (dotted: Johnson 1976) and AMEX (large dots: Frank and McBribe 1989). All curves have been normalized relative to a common precipitation rate of 10 mm day^{-1}. All profiles show a mazimum heating rate above 500 mb except the GATE profile which is near 600 mb.

appropriate parameterizations can be developed for use with satellite observations and coupled models. Thus, it is clear that it is necessary to decrease our high level of uncertainty about convection over the warm pool and the degree to which it is organized. While these studies must be viewed as exploratory, they are highly leveraged by our understanding of mesoscale convective systems at midlatitudes and over the Atlantic.

6) Convection and interfacial fluxes

The heat flux between the ocean and atmosphere is temporally and spatially complex in the region of active convection (cf. Bean and Reinking 1978; Gautier 1978). The smallest scale on which convection occurs is the individual convective cell, which has a space scale of 1–10 km. There are large diurnal cycles in SST when the wind is light (Ostapoff and Worthem 1974), which gives rise to a diurnal cycle in atmospheric convection and in ocean mixing (Price et al. 1986; Moum et al. 1989). The incoming solar radiation is primarily modulated by the diurnal cycle and by the clouds associated with mesoscale convection. There are two types of subsiding air masses, one relatively dry and warm associated with the slow subsidence outside the convection and during its dissipation, and the other cold and moist associated with downdrafts in the convective towers and the subsidence from the stratiform regions of the cluster. What is observed is

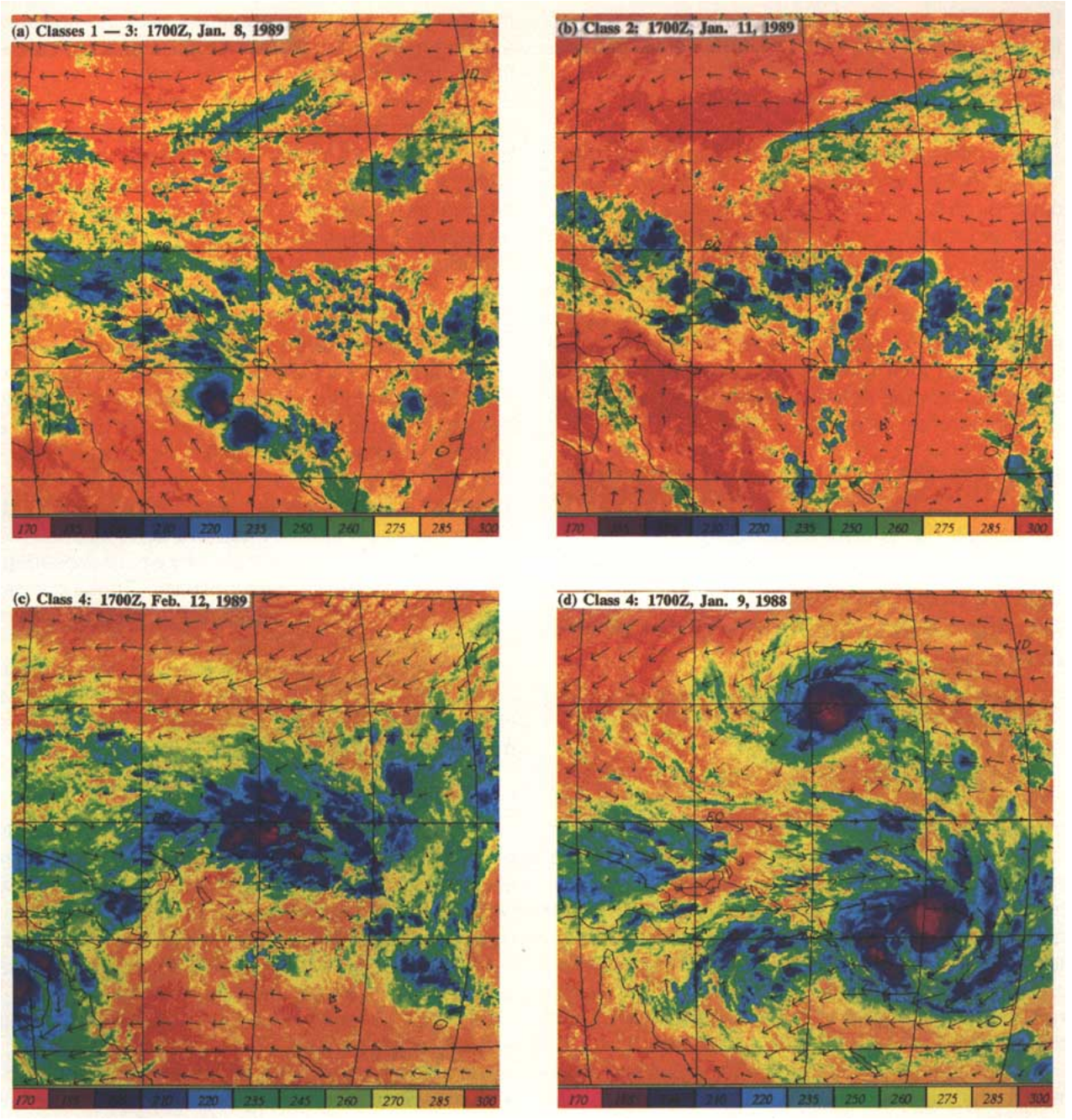

FIG. 9. Four distributions of typical convection types encountered in the western Pacific Ocean. The diagrams show distributions of effective blackbody radiation temperatures relative to the color codes at the base of each panel. The arrows indicate 850-mb wind fields from ECMWF model data. The classes of convection will be referred to later. Figures compile by R. A. Houze, Jr. and Shuyi Chen. (a) Generally undisturbed conditions in a light wind regime. Near the equator, there are a number of small convective elements. The line of convection extending from the equator to the southeast is associated with the Solomon Islands. (b) Relatively disturbed period convective elements of order 100-km diameter between the equator and 10°S. (c) Disturbed period typified by mesoscale and large-scale convective structures along the equator. (d) Synoptic-scale disturbances where mesoscale structures have developed into typhoon intensity. The typhoon pair propagated westward and poleward in their respective hemispheres. Note the strong westerlies over the equator between the cyclone pair, the winds were considerably stregthened by the cyclonic development.

highly dependent on whether the observations are made in the convective cell or in the unstable environment outside of the convective cells. In terms of local fluxes, the cold subsidence in the convective regions is very important, as it severely dilutes the boundary layer in a region of local high winds. The effect is to increase interfacial heat fluxes by almost an order of magnitude compared to regions outside the distur-

bances (Young et al. 1991). In particular, because of the large air–sea temperature difference, an enhancement of the sensible heat flux from the ocean to the atmosphere occurs in the downdraft region (Gautier 1978; Greenhut 1978).

According to the formulation of bulk parameterizations (Large and Pond 1982), the latent heat flux depends on the vapor pressure difference between air at the sea surface temperature and the air above the sea surface, the drag coefficient, and on the wind speed. For the case of no wind, the bulk formula predicts no moisture flux. However, Liu et al. (1979) suggest that this is not the case, and that the exchange coefficient in their formula varies strongly with wind speed at low wind speeds, especially when the air–sea temperature difference is large.

Because the strongest observed equatorial winds occur during westerly bursts, they represent an important forcing mechanism for the upper ocean in the western Pacific.

The heat and moisture flux depends on SST, but changes of SST depend strongly on ocean mixed-layer thermodynamics including the fluxes. The momentum and buoyancy fluxes at the sea surface, combined with the initial ocean-buoyancy profile, determine the evolution of the mixed layer and its heat budget. Thus, precipitation and salinity effects, through their influence on the buoyancy flux and the buoyancy profile, may exert a control on the ocean mixed-layer heat budget (Ostapoff et al. 1973; Miller 1976), and thus on the flux of heat to the atmosphere.

As pointed out above, the fluxes of heat and moisture in the western Pacific warm pool are generally controlled by mesoscale convection, with near-zero net heat flux on time scales longer than about one day (Godfrey and Lindstrom 1988; Lukas 1989; Godfrey et al. 1991). This equilibrium is disturbed by synoptic-scale atmospheric events; it is during these times that heat is effectively extracted from the warm pool by the atmosphere (Meyers et al. 1986; Lukas 1989). The horizontal scales of SST and sea surface salinity variability are controlled by the convective processes and the synoptic-scale forcing.

Scale interactions occur when processes operating on a particular time or space scale modulate the energy of processes on different time or space scales. This can arise only from nonlinear dynamics or thermodynamics. The turbulent fluxes of heat, moisture, and momentum between the upper ocean and the lower atmosphere are nonlinear, and are dependent on one another. Synoptic-scale forcing modulates the atmospheric convection, and thus substantially modulates the air–sea fluxes (e.g., Seguin and Kidwell 1980). It is this synoptic atmospheric forcing that can change the warm-pool system from a nearly one-dimensional radiative–convective equilibrium into a fully three-dimensional system.

b. Impact of atmospheric variability on the ocean

1) Episodic wind events and ocean response

The strong near-equatorial wind events of the western Pacific (see Fig. 7) induce a substantial oceanic response both in the warm pool and remotely in the central and eastern equatorial Pacific (e.g., Luther et al. 1983; Lukas et al. 1984). Episodic wind events force families of waves in the equatorial wave duct. Kelvin waves propagate eastward and influence the eastern Pacific basin, while Rossby waves propagate to the warm pools of the western basin. These internal waves change the sensitivity of the SST to ocean–atmosphere fluxes by changing the thermocline depth, a major factor in entrainment cooling of the mixed layer. McPhaden et al. (1988) and McPhaden and Hayes (1991) specifically address the local and remote impacts of episodic wind bursts.

(i) *Local response*

Because the strongest observed equatorial winds occur during westerly bursts, they represent an important forcing mechanism for the upper ocean in the western Pacific. Local oceanic response consists of dynamic effects and turbulent mixing associated with large momentum fluxes, as well as diabatic effects associated with altered buoyancy fluxes.

The local dynamic response to impulsively applied westerly winds includes an equatorward Ekman convergence with associated downwelling, and the appearance of an accelerating eastward surface current (the Yoshida jet) with its maximum on the equator (Moore and Philander 1977; Cane 1980). This strong flow (speeds in excess of 1 m s^{-1} have been observed) carries warm surface water eastward. If the wind is held steady, equilibrium will be reached after about a week when a zonal pressure gradient is set up across the westerly fetch. However, typical westerly bursts do not last long enough for currents to reach this equilibrium state (Keen 1988), and the response must be described in terms of transient dynamics. McPhaden et al. (1990) and Delcroix et al. (1992) show this for the warm pool during the 1986–87 ENSO episode.

Another dynamic effect of the westerly bursts occurring in the far western Pacific is to raise the thermo-

cline near the boundary through upwelling along the Papua New Guinea coast (Lukas 1988). This upwelling can be intense because the coastline is close to the equator and nearly parallel to the winds.

The diabatic response of the warm pool to a westerly wind burst is poorly known, even though much has been learned about remote effects. Westerly winds of up to 15 m s^{-1} were observed for a three-day period during January 1986 during WEPOCS II. If real, but small, spatial mean variations in mixed-layer quantities are ignored, then the hydrographic station observations can be sorted into pre- and postevent categories. After the event, the mixed-layer depth was doubled (from 22 to 44 m), and the averaged mixed-layer temperature was about 1°C colder compared to before the event (Lukas and Lindstrom 1991). As the spatial scale of the burst was relatively large (approximately 1500 km zonally by 500 km meridionally), it is probable that cooling occurred over a large area of ocean. It is reasonable to surmise that the relatively convection-free weather experienced after the wind event was associated with the cooling. From Fig. 7, we note that convergent regions are associated with the surge. The extended westerly winds behind the surge are divergent and subsident. McPhaden and Hayes (1991) show that evaporative cooling dominated during the westerly bursts that occurred during the 1986–87 ENSO.

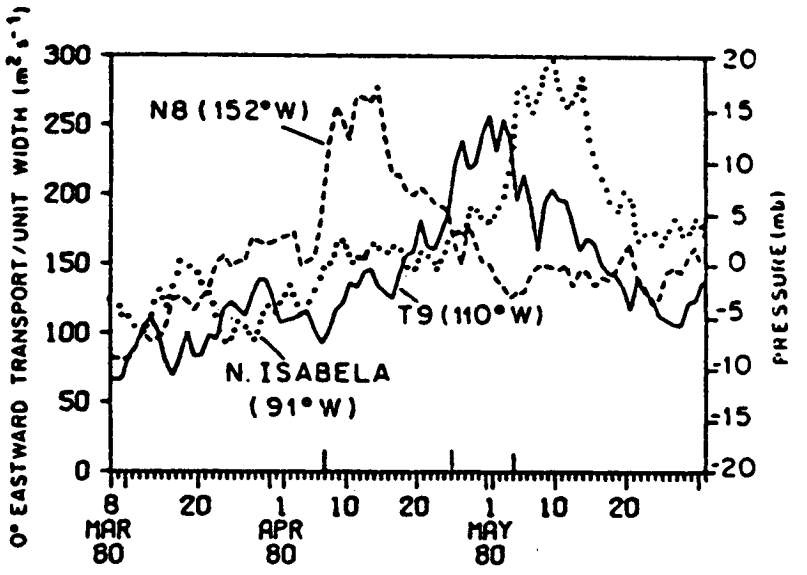

FIG. 10. Oceanic pulse along the equator following an episodic forcing event in the western Pacific Ocean occurring in March 1980. The curves show a time section of the eastward transport per unit width on the equator at 152°W, 110°W and Isabell Island (90°W) in the Galapagos. The three stations are separated by 5000 km and 2000 km, respectively, where records indicate a pulse propagating eastward at about 2 ms^{-1} typical of an oceanic equatorial Kelvin wave. Ensemble of such pulses were observed by Lukas et al (1984) during the onset of the 1982–83 warm event. Diagram from Knox and Halpern (1982).

It is important to note that the dynamic and diabatic responses are not separable; the dynamic response depends on the downward mixing of momentum in the upper ocean, and the thermohaline response of the mixed layer depends on vertical displacements of the thermocline and halocline, which are controlled by the dynamic response (Delcroix et al. 1992). The latter connection is the mechanism by which remote tropical Pacific wind variations influence the mixed-layer temperature and salinity in the warm pool.

(ii) *Remote response*

Equatorial waves carry the influence of wind events outside of the domain of the wind, causing remote variations. Equatorial inertia-gravity, Kelvin, Yanai, and Rossby waves are all possible carriers of the strong wind-event signal to remote regions of the equatorial Pacific (Eriksen et al. 1983). Here, we will concentrate on Kelvin waves, which carry signals only to the east, even though other equatorial waves can also propagate information to the east.

Figure 10 (from Knox and Halpern 1982) shows the eastward propagation (at 2–3 m s^{-1}) of the eastward transport and sea level signal that was generated by the strong April 1980 westerly burst in the western Pacific Ocean. Lukas et al. (1984) observed an ensemble of westerly bursts in the western equatorial Pacific and showed that they generated first and second vertical-mode Kelvin waves during the onset of the 1982–83 ENSO. It was also suggested that these Kelvin "pulses" were actually responsible for a major portion of the mass redistribution that occurred. Because the sea level and zonal current anomalies associated with these Kelvin waves are of one sign, there is a net anomalous eastward displacement of water parcels. Harrison and Schopf (1984), who modeled this process, showed that even though the dynamics of the Kelvin wave pulses are essentially linear, there is a nonlinear interaction of the pulse with the background thermal structure. A sequence of such pulses can produce an evolutionary warming trend. Harrison and Giese (1988) showed that nonlinear dynamics may result in a decay of the first mode and enhancement of the second-mode Kelvin wave; combined with modal dispersion, this effectively results in a prolonged duration of the eastern Pacific warming

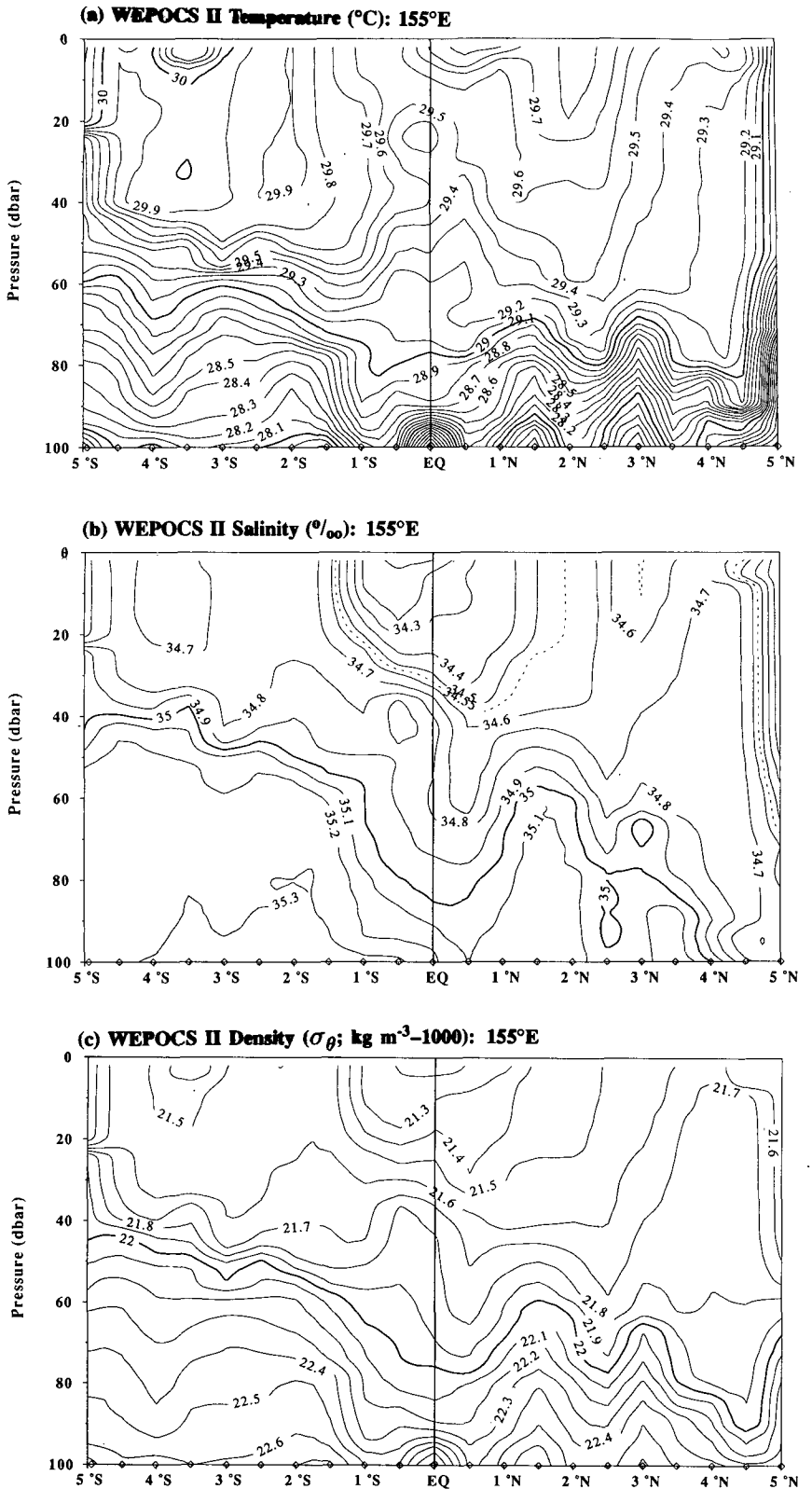

FIG. 11. Cross sections of (a) ocean temperature (°C), (b) ocean salinity (°/₀₀), and (c) ocean density (σ_θ kg m^{-3} – 1000) as a function of depth (1 dbar is equivalent to about 1 m) along the 155° E meridian. Data were collected during the Western Equatorial Pacific Ocean Climate Studies Program (WEPOCS).

associated with a single pulse. In this manner, short time-scale atmospheric variability can cause low-frequency SST anomalies.

In summary, episodic wind events may affect SST in three ways:

- by increased evaporation and sensible heat loss;
- by forcing equatorially trapped ocean Kelvin waves, thus causing advective temperature changes in regions of strong east–west temperature gradients (e.g., Harrison and Schopf 1984; Harrison and Giese 1988); and
- by enhanced mixing between the surface layer and the cooler ocean interior.

For a given surface wind speed u, the above three processes are proportional to u, u^2, and u^3, respectively, so that each process depends very differently on wind-speed variance (Lukas 1988; McPhaden and Hayes 1991). A key issue is, thus, the efficiency of the wind in the forcing of these modes. The response will differ markedly depending on the state of the upper ocean. For example, the flux of momentum into the ocean upper layer will be much greater into a shallow mixed layer than into a deep layer.

2) Freshwater flux and the ocean response

The Western Equatorial Pacific Ocean Circulation Study (WEPOCS; Lindstrom et al. 1987) is one of the few TOGA process studies that has been conducted in the western Pacific. Figure 11, provides some evidence that precipitation, and the resulting freshwater flux from the atmosphere to the ocean, may impact the dynamics of the warm pool. The panels show cross sections (latitude and depth) of T (°C), S (°/₀₀), and density (kg m^{-3} less 1000)

along the 155°E meridian between 5°N and 5°S collected during a WEPOCS II cruise. To the south of the equator, the mixed layer (as defined by the density distributions) is relatively deep. The first pycnocline near 2°–3°S is at 40 m. However, nearer the equator the first pycnocline is much shallower because of a freshwater lens in the first few meters.

The sections show clearly that in the warm pool the mixed-layer depth is not determined by temperature alone but is also a strong function of salinity. Prior to the WEPOCS cruises there was a tacit assumption that the upper ocean was well mixed in both salinity and temperature and much of the monitoring program in TOGA was built around that assumption. Clearly, that is not the case. Figure 11 suggests that there are two generic $T-S$ profiles in the warm pool. Either the column is very well mixed (Fig. 12a) or it contains substantial substructure due initially to the flux of freshwater altering the salinity, and finally due to the reduced mixing and the subsequent heating of the surface water (Fig. 12b). The well-mixed profiles are rather rare and seem to be observed only following westerly bursts. Indeed, the profile shown in Fig. 12b has proven to be the ubiquitous form found in the warm pool (Lukas and Lindstrom 1991).

The variation in salinity shown in Fig. 11b and 12b, created by a downward flux of freshwater, generates a distinct stable layer near the surface. The layer between the base of the mixed layer and the top of the thermocline has been called the "barrier layer" by Lukas (1988) because it acts as a barrier to entrainment cooling of the surface mixed layer. These results have been verified subsequently through additional observations by the French SURTROPAC program and by the United States/People's Republic of China bilateral cruises. Within the barrier layer, wind mixing is restricted so that the regions below the layer are "insulated" from the influence of the atmosphere. In addition, the state of the ocean boundary layer is highly variable and responds strongly to episodic momentum flux as well as variations of the moisture and heat fluxes.

c. Feedbacks

1) POSSBILE SALINITY EFFECTS ON THE ENSO MECHANISM

The concept of the barrier layer, in which isothermal but salt-stratified water effectively insulates the surface layer of the western equatorial Pacific from the thermocline, raises interesting new possibilities regarding the nature of the ENSO instability. This thin surface lens of relatively fresh water appears to slide over the top of the region, responding within days to changes in the winds (Lukas 1988). At present, due to lack of adequate salinity profiles, it is not known how much of the western equatorial Pacific warm pool is insulated by the fresh lens. If it is assumed that the entire warm pool is covered by such a low-salinity lens, then SSTs throughout this region are usually unaffected by oceanic Kelvin and Rossby waves (which influence the thermal structure well below the mixed layer) so that SSTs within the warm pool are affected only by local surface heat fluxes.

In theoretical explanations of ENSO (see Philander 1990), it is generally assumed that Kelvin and Rossby waves may be the only way to provide an "oceanic memory" by which the last ENSO event triggers the next. Given the discussion above of the thermohaline structure, we may now raise another possibility. Is it possible that salinity effects may also provide a long-term memory? This may occur in the following manner. Heavy precipitation in the western equatorial Pacific provides a strong buoyancy flux that tends to freshen and stabilize the surface layer over time, increasing the total buoyancy difference across the barrier layer even though the layer is nearly isothermal. During periods between warm events, there appear to be fewer strong wind events or westerly bursts (see Fig. 7). This same figure also shows that at times of negative SOI (Southern Oscillation index) there are abundant bursts (see Keen 1988; Webster and Chang 1991). Suppose then, that there is little or reduced mixing during these quiet periods between ENSO warm events. The surface waters of the far western Pacific will freshen steadily, and with the freshening the quantity of water above 28°C in the western Pacific Ocean will increase. Prior to the next warm event, the advective response to the increased number of westerly wind bursts will increase the eastward flow of fresher, warmer water along the equator. Because of the barrier layer effect, this stable layer could advect considerable distances before it is mixed with the saltier, colder water below.

Entrainment heat flux estimates made using zonal-wind time series like those in Fig. 7 were presented by Lukas (1988). During the 1982–83 ENSO, the equatorial region near 150°E may have cooled substantially due to entrainment cooling primarily associated with westerly wind anomalies, while the region near the date line had a much smaller entrainment heat flux associated with the event. Because the thermocline was observed to shoal markedly in the western Pacific during this event (Meyers and Donguy 1984), it is very likely that winds were able to penetrate the barrier layer, and that entrainment cooling was activated. The reversal of the zonal SST gradient observed in the region was likely due to this effect; the impact on the stability of the warm-pool system may have been important.

Meyers et al. (1986) show that episodic surface wind events are responsible for significant evapora-

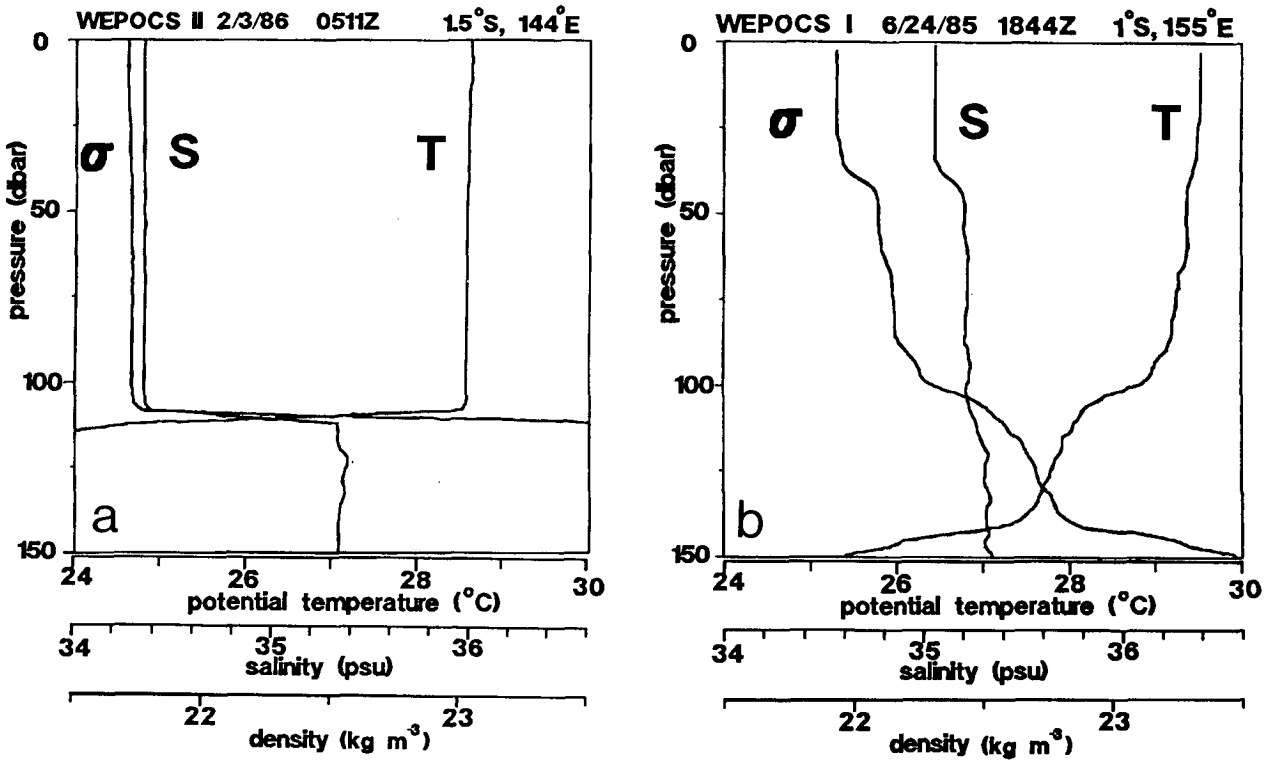

FIG. 12. Examples of temperature (T;°C), salinity (S, ‰), and density (σ: kg m^{-3} − 1000) profiles for (a), a very well mixed upper ocean, and (b) an upper ocean containing considerable substructure in T, S, and σ. The WEPOCS data indicates that the (a) profile is rather rare and only occurs after substantial mixing by sustained westerly bursts. Profile (b), on the other hand, indicates a far more ubiquitous structure: A distinctive fresh lens near the surface induced by the large precipitation in the warm pool (see Fig. 3) and the associated shallow surface warm layer of the structure in the western Pacific.

tive cooling of the warm pool. Estimates suggested that entrainment cooling was not contributing substantially to the cooling most of the time. During the 1982–83 ENSO, however, entrainment cooling was estimated to be 50%–100% of the evaporative cooling.

Following an El Niño, atmospheric forcing of the upper ocean in the warm pool returns to very light trade winds, moderate convection at night, and intense, but brief, squalls, which sometimes release an inch or more of rain per hour. During the COARE pilot experiment (February–March 1990), mixing from squalls was strong, but did not penetrate deeper than about 20 m (Brainerd and Gregg 1991). The puzzle is how this weak forcing can warm the upper ocean so that it is nearly isothermal in the upper 100 m but strongly stratified by increasing salinity between 50 and 100 m. The nearly uniform temperature implies vertical mixing, but the salinity gradient demonstrates lateral advection. Consequently, the response to westerly bursts is only one part of the ENSO cycle of the warm pool, and a full understanding of the dynamics of the warm pool requires determining the balance of vertical mixing and horizontal advection when westerly bursts are not present (Chen and Rothstein 1991).

Within the context described above, the warm pool acts as a capacitor whose charge (heat capacity) increases between ENSO events. The ocean influence on the atmosphere is primarily through the remote forcing of the thermocline depth and heat content and the effect of those on the sensitivity of SST to air–sea fluxes, which, in turn, influences local atmospheric variability. Though these ideas are very speculative, they are introduced here to illustrate how the barrier layer and the role of hydrology and salinity may require a qualitative change of ideas about how ENSO works. More observations of the thermohaline structure of the warm pool are needed to test hypotheses such as the one raised above, to map the spatial and temporal variation of the barrier layer, and to determine the processes maintaining the barrier layer.

2) Estimates of the warm-pool energy balance

Niiler and Stevenson (1982) used climatological datasets to infer the heat balance of the warm pool. They concluded that entrainment cooling provides 22 (30) W m^{-2} average for the region enclosed by the 28° (29°)C isotherm. Because the haline structure of the warm pool seems to prevent entrainment cooling

much of the time (Godfrey and Lindstrom 1988), either the net surface heat fluxes used by Niiler and Stevenson are too large, or the entrainment cooling occurs only episodically, such as during wind bursts or ENSO events. Both of these explanations are likely, as explained below.

Wyrtki (1965), Esbensen and Kushnir (1981), Weare et al. (1981), Hsiung (1985), and Reed (1985) all give maps of the annual mean net heat flux into the Pacific Ocean, estimated from marine climate data using various empirical formulas for the radiative fluxes and the sensible and latent fluxes. In the equatorial western Pacific Ocean, their values range from about 20 W m^{-2} (Esbensen and Kushnir 1981) to 100 W m^{-2}. This large range of estimates results, perhaps, from using data from different time periods, but the major cause is probably from the use of different empirical formulas for the calculation of fluxes (cf. Blanc 1985; Molinari and Hansen 1987). There is also ample evidence of observational problems in the climatological dataset; for example, the climatological air–sea temperature difference is roughly 0.5°C in the warm pool (Esbensen and Kushnir 1981); recent high-quality observations uncontaminated by ship heating influences and flow distortion suggest that the difference may be more like 1°–2°C (Lukas 1989).

The problem of vastly different flux estimates has substantial implications for the feasibility of successful coupled ocean-atmosphere models. For example, if the mean net heat flux supplied to a model is in error by 40 W m^{-2} and other components of the fluxes are correct, the model will predict that a mixed layer with a typical depth of 50 m will change temperature at a rate of about 6°C yr^{-1}. Such magnitudes are greater than those observed in ENSO transitions. Anderson and Gordon (personal communication) note that in the 16-layer Cox Ocean GCM coupled to the 11-layer U.K. Meteorological Office Atmospheric GCM, an El Niño event was generated by such spurious warming. Gordon and Corry (1991) has shown for this ocean model that the net heat flux into the western equatorial Pacific must be close to zero. The algorithms used to calculate the components of the net heat flux should all be checked explicitly in the equatorial west Pacific to minimize such spurious effects.

d. Some key uncertainties

The description of atmospheric and oceanic processes in the warm-pool regions as presented above is clearly incomplete. In many aspects, our ability to model the warm-pool region, or the tropical ocean in general, rests on the completeness of that description. For example, without a better depiction of the warm pool, parameterizations of interface fluxes and the ocean and atmospheric responses to the fluxes will remain inadequately described. The need to increase our knowledge of the warm pool is underlined by a number of key uncertainties discussed below:

- The tropical atmosphere is sensitive to small variations in sea surface temperature. Such sensitivity is exaggerated in regions of warmest sea surface temperature.

Because there is a nonlinear relationship between SST and latent heat flux, the western Pacific warm pool is a region of enhanced sensitivity of the atmosphere to small changes in the ocean. Thus, errors in estimating the warm-pool SST will severely limit our ability to forecast the state of the coupled ocean–atmosphere system on several time scales. This belief originates from a number of experimental results using atmospheric general circulation models that were forced with constant SST distributions characteristic of different phases of the ENSO cycle. For example, Palmer and Mansfield (1984) have shown that a stronger atmospheric perturbation occurs during the ENSO cycle when the SOI is positive rather than negative, and when the warm regions of the western Pacific Ocean are slightly warmer than normal. These results have proven to be robust, as other GCMs (e.g., Geisler et al. 1985) have produced similar sensitivities.

. . . there appear to exist a number of important gaps in our knowledge of the coupled ocean–atmosphere system that have been exposed through the TOGA program.

On a longer time scale, understanding the processes that regulate SST in the warm-pool region is of crucial importance for predicting the global response to forcing from increased atmospheric loading of greenhouse gases. Modest changes in SST in the warm pool may alter the temperature-dependent capacity of the ocean to absorb CO_2, and may lead to dramatic changes in the global circulation, including the intensity and frequency of El Niño (Meehl and Washington 1986) and tropical cyclone development.

In summary, small changes in the warmest regions appear to invoke larger climate responses than greater changes in cooler water; however, it is not entirely clear how this sensitivity depends on the time and space scales of SST variability.

- The variation of fluxes between the ocean and the atmosphere is very sensitive to the choice of parameterization, especially in low wind regimes, which are common in the warm pools.

The sensitivity of atmospheric models to even minor variations of SST has been proposed to be a Clausius–Clapeyron effect (Webster 1991). If this is the case, one would expect a similar sensitivity in the surface fluxes in the warm-pool regions. In a recent study, Miller et al. (1992) showed this to be the case. They suspected that previous parameterizations of surface fluxes low wind regimes with speeds below 5 m s^{-1}, which resulted in a very weak coupling between the ocean and the atmosphere. By modifying the transfer coefficients to bring them into accordance with empirical scalings for free convection, dramatic changes in the ocean–atmosphere coupling occurred in the warm pools. The relatively minor changes to the flux parameterizations introduced by Miller et al. resulted in a much stronger coupling between the ocean and the atmosphere and, in general, a better simulation of tropical phenomena.

- The sea surface temperature of the tropical warm pools is very sensitive to changes in the state of the overlying atmosphere.

In models, the SST of the western Pacific warm pool is very sensitive to small changes in the surface heat fluxes, even when possibly large salinity effects are ignored. Gent (1991) used a primitive equation model of the Pacific to show that when the minimum wind speed for computation of latent fluxes (a parameterization of short time-scale variability) was reduced from 4 to 3 m s^{-1}, the net heat flux into the warm pool increased from 13.5 to 18 W m^{-2} and SST went from 29.5° to 32°C. Seager et al. (1988), using a simpler ocean model, show that the sensitivity of SST to changes in net heat flux is about 1°C per 12 W m^{-2}. It seems important to develop a method for calculating explicitly what this minimum wind speed should be, based on physical considerations that take into account possible temporal and spatial variability of the mesoscale convection that gives rise to it.

- Although theories of low-frequency variability of the coupled ocean–atmosphere system depend crucially on the form of the basic state of the warm-pool region of the tropical Pacific Ocean, the processes that determine and maintain the basic state are not understood.

The warm pool has the highest SST and the most intense atmospheric convection anywhere in the open ocean. The two basic theories of the El Niño–Southern Oscillation phenomenon (i.e., either coupled ocean–atmosphere instability or cyclic equilibrium of a closed tropical ocean basin involving successive boundary reflections and interactions of equatorially trapped modes) depend on the existence of a basic state with very specific properties. The mechanisms that maintain the basic state are not well understood.

The implications are rather clear. Accurate climate simulation with either stand-alone oceanic or atmospheric models will require very precise specifications of interface fluxes (or winds, temperature, and humidity in the atmospheric boundary layer) on one hand, and sea surface temperature on the other. Progress with coupled models will require precise modeling of the physical processes of the coupled system that produce the sea surface temperature distribution which, in turn, requires emphasis on the observing and modeling of the warm-pool regions of the tropical oceans where the greatest errors in estimation and sensitivities exist. While there is considerable evidence that the generation of eastward-propagating oceanic waves is related to the episodic nature of warm-pool meteorology, there are serious gaps in our knowledge of which atmospheric processes produce the forcing.

The processes that accomplish the phenomenological organization or interaction over a wide temporal range are not clearly defined. Nor is it obvious how important the low-frequency variations are in comparison to the higher-frequency episodic events in perturbing the ocean structure through modification of heat, moisture, and momentum fluxes between the ocean and the atmosphere. Finally, the impact of the coupled tropical ocean phenomena on the global climate system during all phases of ENSO is still not well understood.

In summary, there appear to exist a number of important gaps in our knowledge of the coupled ocean–atmosphere system that have been exposed through the TOGA program. TOGA COARE was proposed to work toward the resolution of these scientific problems.

3. Scientific objectives and strategies of TOGA COARE

a. The scientific objectives

Considerable discussion and planning have led to the concept of TOGA COARE, the scientific goals of which are to describe and understand:

1) the principal processes responsible for the coupling of the ocean and the atmosphere in the western Pacific warm-pool system;

2) the principal atmospheric processes that organize convection in the warm-pool region;

3) the oceanic response to combined buoyancy and wind-stress forcing in the western Pacific warm-pool region; and

4) the multiple-scale interactions that extend the oceanic and atmospheric influence of the western Pacific warm-pool system to other regions and vice versa.

Collectively, the goals of TOGA COARE are designed to provide an understanding of the role of the warm-pool regions of the tropics in the mean and transient state of the tropical ocean–atmosphere system. Goal 1 has the highest priority, as it speaks directly to the coupling of the ocean and atmosphere in the warm pool itself. This goal will lead to improved parameterizations of heat, momentum, and freshwater fluxes between ocean and atmosphere, which are required for better performance of short- and long-term oceanic and coupled climate prediction models. Goals 2 and 3 are of equal priority. While it is recognized that the atmosphere controls the interfacial fluxes to a greater degree than the ocean in this region, the magnitude and sign of feedbacks depend on processes in both fluids. These goals address the atmospheric and oceanic processes that extend the interfacial fluxes into the interior of each fluid locally. Goal 4 is important for placing the western Pacific air–sea interaction in general, and COARE specifically, firmly in the context of TOGA.

b. Strategy

Some aspects of the COARE goals will be met with new observations. However, many aspects require experimentation with substantially better coupled models. Thus, a practical objective of the observational component of COARE is to improve models.

As TOGA COARE is, ostensibly, an ocean–atmosphere interaction experiment, the principal concentration will be on the oceanic–atmospheric interface. For organizational purposes, however, it is convenient to consider COARE in terms of components. These are:

- An *interface component,* in which the major emphasis will be the measurement and modeling of the interfacial fluxes between the atmosphere and the ocean over a wide variety of atmospheric and oceanic conditions.
- An *atmospheric component,* where the emphasis is on the measurement and modeling of those processes that determine the state of the atmospheric boundary layer, and, thus, influence the interfacial fluxes of heat, water, and momentum. It is anticipated that there will be observations taken over a full extent of weather conditions, ranging from the undisturbed trade-wind boundary layer to the disturbed boundary layer within a convective complexes.
- An *oceanographic component,* where the emphasis is on the measurement and modeling of the response of the upper ocean in order to assess the response to the varying fluxes at the interface that occur over the range of weather events and types encountered in the warm pools of the tropical oceans.

Through these components, TOGA COARE will produce long-term time series of atmospheric and oceanic data collocated in a region (the COARE domain) possessing a representative distribution of warm-pool phenomena in order to approach the goals of the experiment. To achieve concomitant time series, an overlapping observational technique is used in which each scale of atmospheric and oceanic system is overlain by a larger, although less dense, observational network. The larger-scale networks provide a context for the higher-frequency and higher-resolution data.

Central to the plans of TOGA COARE is an intensive observation period (IOP), which will provide a high-quality heat, moisture, and momentum flux dataset of the ocean–atmosphere system in the warm pool of the western Pacific Ocean using diverse observation platforms. These observations will consist of a synergistic mix of concurrent in situ measurements and remote satellite observations over a 4-month period, which is embedded within the enhanced monitoring effort of the World Weather Watch (WWW) and TOGA to ensure that the context of the IOP is known, and that the results of the IOP can be extended to ENSO time and space scales.

The resulting high-quality dataset will be used to characterize and quantify the processes of interaction between the ocean and the atmosphere in the warm-pool regions and the relationship of the warm-pool structures to the larger-scale context. The data will allow the calibration of satellite retrieval algorithms and will provide ground truth for rainfall, surface wind, sea level height, and other ocean–atmosphere parameters in the western Pacific Ocean for programs such as the Global Precipitation Climatology Project (GPCP), the NASA Tropical Rainfall Measurement Mission (TRMM), TOPEX/Poseidon, and NSCAT.

The dataset will be extremely useful for the initialization and validation of coupled models. It is also clear that the COARE dataset will identify model weaknesses. For the reasons described above, we add a fourth component to TOGA COARE that transcends the observational phase: the modeling component.

4. Scientific objectives of the COARE components

Relative to the general goals of TOGA COARE discussed in the last section, there are specific scientific objectives for each of the components. These objectives will be used to define an experimental design that will be discussed in section 5.

a. The interface component

The scientific objectives of the interface component of TOGA COARE are:

(i) to provide a high-quality dataset of heat, moisture, and momentum fluxes in the warm-pool region;

(ii) to understand the physics and thermodynamics of interfacial exchange processes that have particular behavior in this region of low wind speeds and strong atmospheric convection;

(iii) to improve various empirical formulas used to estimate net surface heat flux for use in the warm-pool regions;

(iv) to determine the magnitude (and significance for longer-term models) of short time-scale variability of the fluxes of heat, moisture, and momentum—hourly, diurnal, and episodal, and;

(v) to understand the impact of the full range of wind structures, from the ambient trade-wind regime through the episodic westerly bursts, on the ocean–atmosphere fluxes of heat, moisture, radiation, and momentum.

All of the scientific objectives listed above fall within the highest category of priority of TOGA COARE. Each contributes to the primary goal of defining the principal processes responsible for the coupling of the ocean and the atmosphere.

b. The atmospheric component

In the context of the goals of COARE, the specific scientific objectives of the atmospheric component are:

(i) to determine the structure of the synoptic and mesoscale components of the large-scale, slowly varying atmospheric circulation in the warm pool—in particular, to determine the morphology of the most convective stage of the 30–60-day mode and its subcomponents;

(ii) to determine the relationship of the phenomena described above to the heat, moisture, and momentum fluxes at the ocean–atmosphere interface in an attempt to relate the atmospheric phenomena of the western Pacific Ocean region to transitions in the dynamics and thermodynamics of the upper-ocean structure;

(iii) to determine the morphology of episodic westerly burst phenomena, including their source, whether in situ or remote;

(iv) to determine the vertical heating distribution and life cycles associated with synoptic events and mesoscale convective cluster components, and compare these results to those from other regions in the tropics;

(v) to determine the character of large-scale, seasonally varying atmospheric circulation of the western Pacific Ocean region, including the detailed surface wind field and its relationship to planetary-scale phenomena;

(vi) to determine the transition of the tropical planetary boundary layer from the descending regions of the eastern Pacific Ocean to the convective western Pacific Ocean region, and to identify when the domain shifts from easterly to westerly during, for example, westerly wind bursts;

(vii) to determine the manner in which motions created by episodic and mean heating in the warm-pool regions transmit their signal to other regions of the tropics and globe, on time scales ranging from weeks to years; and,

(viii) to apply the knowledge gained from the pursuit of the objectives above to improvements in operational forecasting models and global climate models.

These objectives are listed in terms of priority relative to the overall scientific objectives of TOGA COARE. Objectives (i) and (ii) are of primary importance to the first objective of COARE, (iii) and (iv) relate to the phenomenology of convection in the tropics in general, and (vi) and (vii) relate to the extension of these phenomena to the larger global domain. It is believed that the last objective, (viii), which parallels the ultimate objective of TOGA, can be achieved only through a successful investigation of all of the other objectives.

c. The objectives of the oceanographic component

The scientific objectives of the oceanographic component are:

(i) to determine the space–time structure of SST and sea surface salinity (SSS) in the western Pacific warm pool;

(ii) to determine the processes that contribute to SST and SSS variability on time scales of days to months to years in the warm pool;

(iii) to determine how mixing of heat, salt, and momentum occur in the upper-western tropical Pacific Ocean;

(iv) to determine what far-field processes affect the upper ocean in the warm pool, and vice versa; and,

(v) to determine the net mass, heat, and salt flux into the COARE domain.

The objectives are listed in terms of the priorities given by the overall goals of TOGA COARE. Objectives (i) and (ii) are of the highest priority for the first goal of COARE, and (iii) addresses the third goal of

COARE. The oceanographic aspects of the fourth goal, the influence of remote effects on the warm-pool regions, are addressed by (iv) and (v).

d. Objectives for COARE modeling

A number of modeling themes are highly applicable to TOGA COARE:

- **Ocean mass balance:** Development of ocean models is necessary to assess the mass balances of the western Pacific warm pool, the Indo–Pacific throughflow, and western-boundary reflections.
- **Hydrological cycle and salinity:** It is important that models can assess the complete hydrology cycle in the warm-pool regions. Models must be able to diagnose the sources and sinks and the transport of moisture into the warm pool. In addition, models must be able to include the impact of freshwater flux on the buoyancy of the upper ocean.
- **Mixed-layer formulations:** Due to the sensitivity of the heat budgets of the warm pools, it is necessary that mixed-layer formulations be improved to allow for three-dimensional effects, in addition to detrainment of water from the mixed layer. Given the sensitivity of the warm pools to changes in insolation, a more complete treatment of the spectral radiation attenuation in the upper ocean is required. Current models do not differentiate in attenuation even between the long- and short-wave streams, but rather assume, incorrectly, a common attenuation depth for both.
- **Precipitation, cloud clusters, and large-scale circulation:** The sensitivity of the warm pool to variations in the freshwater places considerable requirements on atmospheric models in their simulations of the distribution and intensity of precipitation. Thus, model studies of spatial and temporal variations of precipitation are highly desirable. Furthermore, it is important that the relative roles of radiational and latent heating be assessed as they pertain to convection in general and to superclusters, westerly wind bursts, and intraseasonal variability such as the 30–60-day oscillation in particular.
- **Air–sea fluxes:** With the data from TOGA COARE, it will be possible to apply fairly stringent testing criteria for existing coupled models for latent, sensible heat fluxes and to momentum fluxes. There is critical need for the development of techniques for the assimilation of in situ flux data and data obtained remotely from satellite.
- **Context experiments:** Figure 2b shows that the warm-pool region of the tropical oceans extends well beyond the limits of the western Pacific Ocean. Whereas there are very sound reasons for choosing the Pacific site for the COARE IOP, other warm-pool regions (especially the eastern Indian Ocean) are also centers of intense convection that influence the global climate. As it is unlikely that COARE will be repeated in another basin, it will be up to models to extend the knowledge gained in COARE to other basins. The COARE dataset and the ensu-

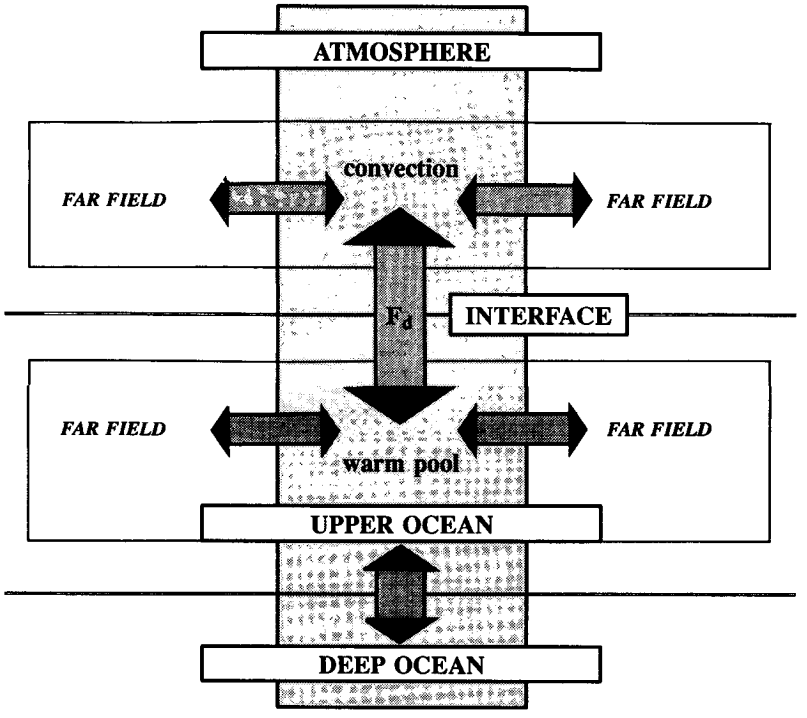

FIG. 13. Schematic representation of the experimental design of the intensive observation period (IOP) of COARE. The shaded vertical box, which links the ocean and the atmosphere, is the intensive flux array (IFA), which is at the center of the COARE large-scale domain (LSD). The IFA represents the zone of maximum oceanographic and meteorological observational intensity where the majority of the resources of the experiment will be focused and where the interfacial fluxes (F_d) will be determined. Within the LSD, surrounding the IFA, is an outer sounding array (OSA) and embellished World Weather Watch aerological sounding and TOGA TAO buoy networks. These networks will be used to determine the transmission of signals into and out of the IFA and to provide a larger-scale and longer-term context for the detailed obervations taken inside the IFA.

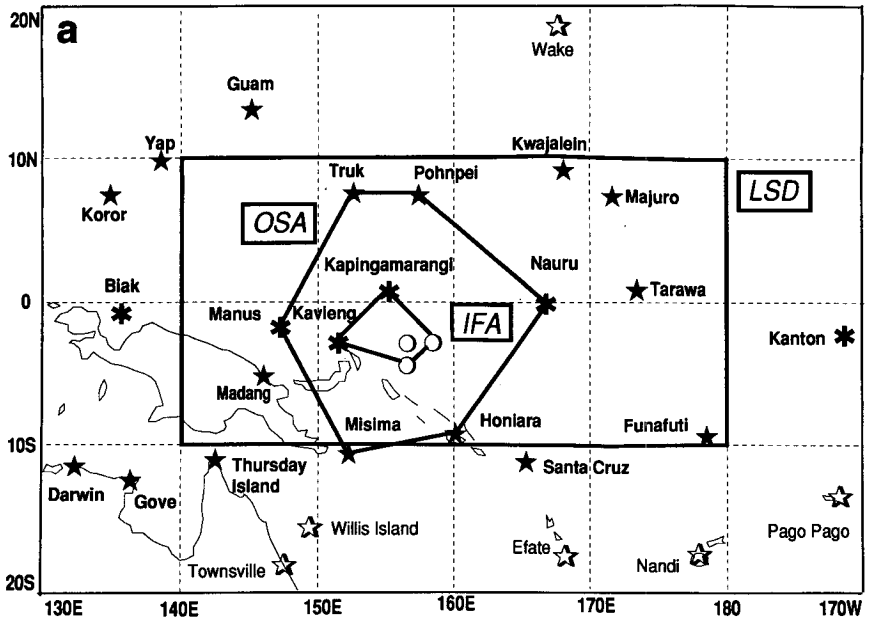

FIG. 14. Composite structure of the intensive observation period (IOP) of TOGA COARE. The legends beneath the panels refer to the symbols used to represent the observational platforms. (a) The entire COARE Domain. The large-scale domain (LSD), the outer sounding array (OSA) and the intensive flux array (IFA) are outlined. Symbols used in the diagram are shown in the attached legend. The figure presents a horizontal depiction of the schematic design shown in Fig. 13.

ing model development point directly toward studies that will allow assessments of the role of the tropical oceans in their entirety on the global climate.

- **Data assimilation:** The TOGA COARE dataset will offer the opportunity for experimentation of assimilating finescale data into operational models and their nested mesoscale subsets. The dataset can serve as the reanalysis standard for convection in the warm pool.

5. Experimental design

a. Overview of the intensive observation phase of COARE

During the last year, an experimental design has been refined to form an observational framework for TOGA COARE. In this section we summarize the most important features of the design and the anticipated achievements during the experiment. Figure 13 shows a schematic representation of the TOGA COARE experimental design. The vertical box represents the zone of maximum concentration of effort and resources for all components of the experiment. This innermost domain is referred to as the intensive flux array (IFA). The principal aim of the IOP is to determine the interfacial fluxes (i.e., F_d) within a relatively small area of the warm pool and to understand the atmospheric and oceanic context of these fluxes. Simultaneously, the response of the ocean will be carefully monitored within the vicinity of the atmospheric forcing. The larger-scale networks that surround the COARE will be used to determine the transmission of the signals to and from the larger-scale, or far-field, atmosphere and ocean.

TOGA COARE will take place in the western Pacific warm-pool region between 20°N and 20°S, bounded by Indonesia on the west and the date line on the east. Within this broad region are the three principal COARE domains:

- **The COARE large-scale domain:** The region 10°N to 10°S and 140°E to 180°. The region has been chosen because it contains the warmest water, is the most convectively disturbed, and receives the greatest amount of precipitation in the tropical Pacific Ocean.
- **The COARE outer sounding array:** The outer sounding array is defined within the large-scale domain by the meteorological sounding stations Truk, Ponape, Nauru, Honiara, Misima, and Kavieng.
- **The intensive flux array:** The IFA is centered at 2°S, 156°E and bounded by the polygon defined by the meteorological stations of Kapingamarangi and Kavieng and ships located near 2°S, 158°E and 4°S, 155°E. A third ship will be located near the center of the IFA (2°S, 156°E). The majority of the meteorological and oceanographic observations will be conducted within the IFA.

The IOP will commence on 1 November 1992 and continue through February 1993. The IOP will be surrounded by an atmospheric enhanced monitoring period, which will commence on 1 July 1992 and continue for one year, and an oceanic enhanced monitoring from September 1991 through October 1993.

Figure 14 represents a composite of the COARE observational network. The central panel (a) shows the entire COARE region. The perimeters of the large-

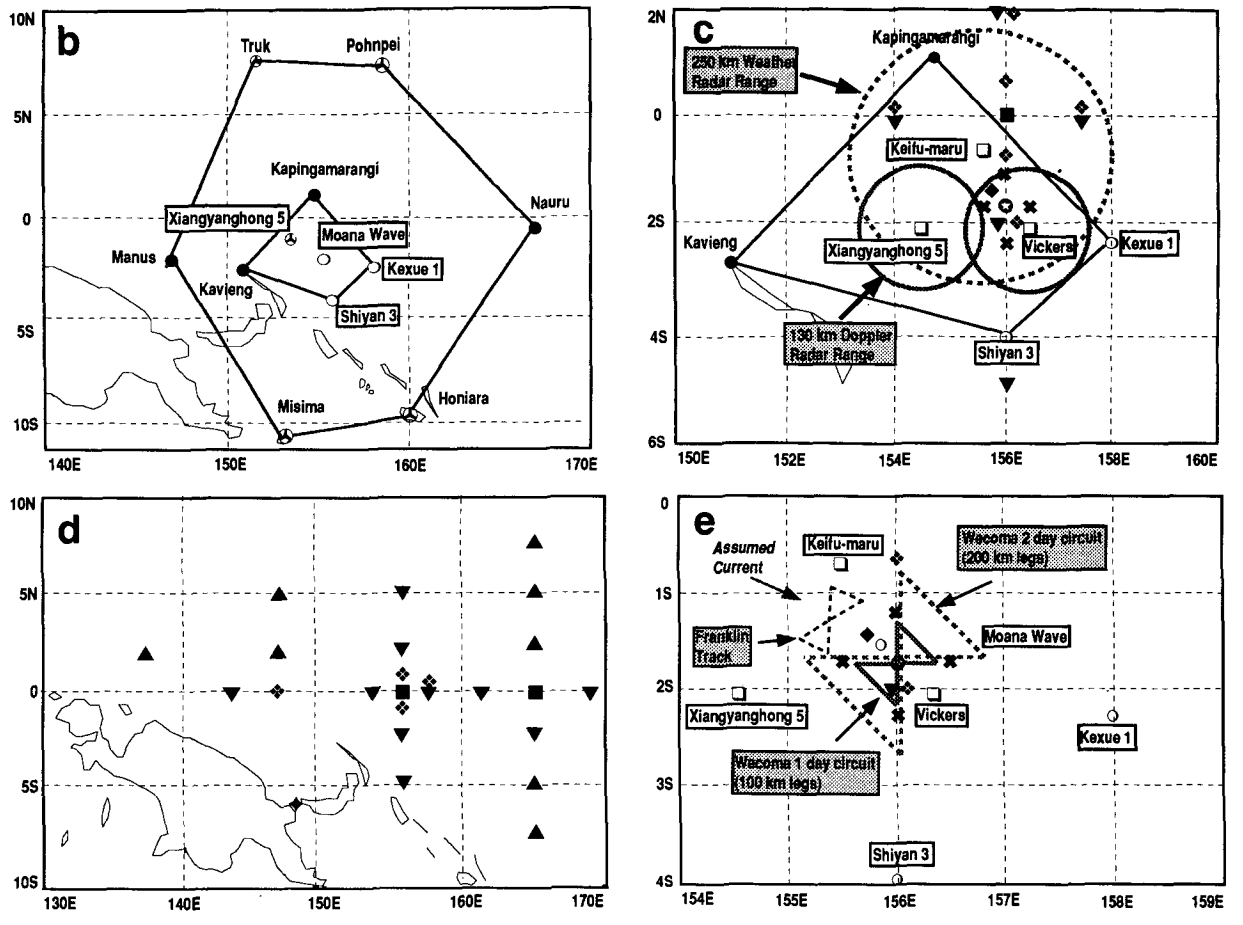

Legend: ❑ - *Radar Vessel* ○ - *ISS Vessel* ● - *ISS Land Site* ✇ - *Rawinsonde Site* ✪ - *IMET Mooring* ▲ - *Atlas Mooring (Temperature only)* ▼ - Atlas Mooring *(Temperature and Conductivity)* ❖ - *ADCP Mooring* ✖ - *Proteus Mooring* ■ - *Acoustic Mooring* ◆ - *PCM Mooring* ✦ - *Vitiaz Strait Mooring*

FIG. 14 (continued). Composite of the intensive observation period of TOGA COARE: (b) The distribution of the observational components within the OSA. The OSA is made up of five rawindsonde systems and an ISS on Nauru. Within the OSA are six ISS sites: three shipborne on the Moana Wave, Kexue 1, and Shiyan 3 and three land based on Kapingamarangi, Manus, and Kavieng.(c) The locations of the ship-borne radars on Xiangyanghong 5, Vickers and the Keifu-maru relative to the oceanographic moorings in the IFA. The former two radars possess Doppler capability. The radars are located to provide near-continual estimates of precipitation over the moorings adn the oceanographic survey ships. On occasion, Vikers and Xiangyanghong 5 will relocate within 50 km to undertake dual-Doppler measurements (d) The large-scale oceanographic moorings comprised of the TOGA TAO and COARE moorings. Additional current moorings are located in the Vitiaz Strait between Papua New Guinea and New Britain. The TAO moorings are part of an array which stretched across the Pacific Ocean with mooring lines between 8°N and S every 15° longtitude. The TAO will provide much of the oceanographic far-field coverage for COARE in the equatorial waveguide. (e) The oceanographic survey cruises within the IFA. The patterns refer to tracks and circuits of the oceanographic ships as described in the text.

scale domain and the outer sounding array of COARE are outlined in panel a. The solid diamonds refer to WWW radiosonde stations. The solid and open circles show the locations of the special COARE ground-based and ship-based ISS systems, respectively. An ISS is a composite of observing systems, including a 915-MHz wind profiler, an omega-sonde system, a radio acoustic sounding system (RASS), which measures the vertical profile of virtual temperature, and a surface meteorology system including a suite of radiometers. Panel b of Fig. 14 shows the distribution of the sounding systems in the outer sounding array and the IFA. Panel c shows the locations and ranges of the radars within the IFA, together with the locations of oceanographic moorings in the IFA. Two Japanese radars are also located on Manus Island. Panel d plots the location of all of the COARE moorings, including the TOGA TAO ATLAS moorings. The moorings will form the basis of the enhanced oceanographic monitoring of COARE. A further long-term context for the COARE oceanographic measurements comes from the Volunteer Observing Ship (VOS) Expendable

TABLE 1. Listing of the ships involved in TOGA COARE during the IOP. The solid lines show the periods when the ships will be on location in the IFA. The lettering indicates the ports of call: Honiara (NIR), Guam (GUM), Rabaul (RAB), Kavieng (KAV), Townsville (TSV), Pohnpei (PNI).

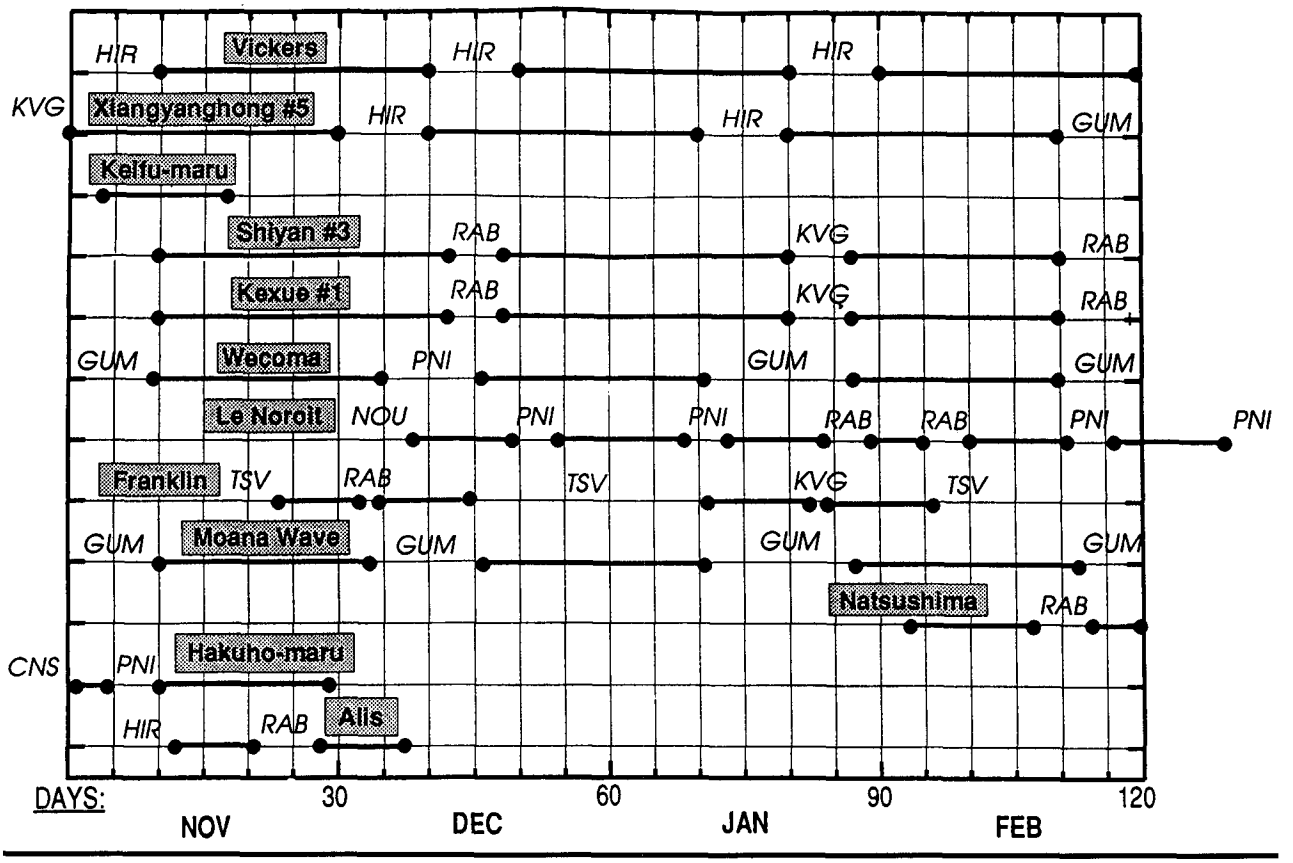

Bathythermograph (XBT) program and the TOGA/WOCE drifting buoy program, both of which are integral parts of the TOGA program. Finally, panel e shows the paths of the oceanographic survey cruises within the IFA.

A list of the ships taking part in COARE, together with their schedules, is given in Table 1. The Vickers and the Xiangyanghong 5 will be located in the IFA and support the surface-based Doppler radars (panel c, Fig. 14). The Keifu-maru will also carry a weather radar and will be located in the northern part of the IFA during the first part of November. The Vickers and the Xiangyanghong 5 will be on location in the IFA for most of the IOP. The Shiyan 3 and the Kexue 1 are principally meteorological ships carrying ISS's at the eastern and southern points of the IFA (panel b, Fig. 14). The Moana Wave will also carry an ISS and, together with the remainder of the ships, will engage in ocean-mixing and air–sea flux research in the vicinity of the IFA.

Figure 14 (panels c, d, and e) show a number of different types of oceanographic moorings. Table 2 describes the function of each type of buoy. Collectively, the buoys provide subsurface temperature and salinity profiles (ATLAS, PROTEUS), ocean-current profiles (PROTEUS, ADCP, PCM), surface meteorological measurements (ATLAS, PROTEUS, IMET), and sea state (acoustic mooring). The PROTEUS and IMET measure components of the surface radiation and, together with the acoustic moorings, estimate rainfall.

Table 3 lists the satellite remote-sensing instruments that are likely to be available during the IOP of COARE. The table shows the satellite and the sampling frequency, the instruments and their resolution, and the parameters retrieved. The COARE domain is within view of the Japanese Geostationary Meteorological (GMS), and the NOAA, ERS-1, TOPEX/Poseidon, and DMSP orbiting satellites. The large circles on panel a of Fig. 14 show the direct readout areas for the AVHRR LAC (local area coverage), which has a 1-km resolution. The communication hubs for the LAC data are Guam, Kwajalein, and Townsville. The AVHRR GAC (global area coverage) will also be available from NOAA archives. The utility of the satellite observations for the three observational

components of COARE will be discussed in ensuing sections.

Table 4 shows the seven aircraft that will take part in the COARE IOP. The tentative schedule, the range of operating altitudes, and the number of hours available for research during the IOP are listed. The NOAA WD-P3's and the NCAR Electra will operate out of Honiara. The NASA DC-8 and the UK C-130 will stage out of Townsville, Australia, together with the NASA ER-2 aircraft. The Australian Cessna will operate out of Kavieng.

The primary operations center for the IOP will be at Townsville, Australia. A second center will be maintained at Honiara, Solomon Islands (panel a, Fig. 14). Honiara represents the closest major airfield and communications hub to the IFA and will support the majority of the turboprop aircraft operations.

A sophisticated communication network will be in use in the TOGA COARE region. The network is designed to take care of the day-to-day running of the experiment and also for the real-time transmission of selected COARE field-data using the Global Telecommunications System (GTS). Communication occurs between the three COARE hubs: the Townsville Operations Center (TSV), the Honiara Operations Base (HIR), and the observational platforms (the ships, sounding sites, aircraft, and radars).

b. The design of the interface component

1) General observational strategy

High-quality estimation of air–sea fluxes of sensible heat, latent heat, and momentum are a critical element of TOGA COARE. The measurement and subsequent parameterizations of these fluxes will provide, simultaneously, the surface forcing at the top of the ocean and at the bottom of the atmosphere. Besides the magnitude of the fluxes, their spatial and temporal variability needs to be measured. On small scales, the fluxes are very intermittent, due to the fundamental nature of turbulence. On larger scales, features such as horizontal SST gradients can cause large variations in the averaged fluxes due to the changes in stability of the air over different water temperatures. As the fluxes connect the upper ocean and the lower atmosphere, and are thus the local mode of communication between the two spheres, interface measurements have the highest priority in COARE.

2) Specific observational strategies

There is no dominant method of measuring ocean surface fluxes to the accuracy and at all the resolutions desired to meet COARE objectives. Thus, the prudent approach is to estimate the fluxes with a number of different methods for comparison and synthesis. Fluxes inferred from spaceborne sensors and calculated from large-scale numerical models will monitor the far-field responses and provide the large-scale coverage. It is expected that these will improve with time as the impact of COARE data are felt. Fluxes measured from ships and aircraft during the IOP will provide finer-scale temporal and spatial details. Measurements by the direct eddy correlation method on ships and aircraft will serve as one type of standard to compare with fluxes derived by other methods. The closures on atmospheric and oceanic budgets will serve as additional tests. Flux packages installed on long-term moorings will provide observations both forward and backward in time from the IOP so that long time series and climatology patterns can be constructed.

Top priority will be given to the development of parameterization schemes under the low mean wind and highly convective regimes in the western Pacific. Such parameterization methods are needed to link the microscale turbulent fluxes to the more ready available macroscopic parameters such as wind, temperature, and humidity measured on buoys and ships and

Table 2. Description of the oceanographic buoys used in the IOP. The first column shows the name of the buoy, which may be cross-referenced with Fig. 14. The second column shows the measurements that will be made by each buoy type.

Type of mooring	Measurements
ATLAS	Wind speed and direction Air temperature, relative humidity, SST Subsurface temperature (to 500 m) SEACAT conductivity and temperature recorder(s)
PROTEUS	Wind, air temperature, relative humidity, SST Vertical profile of ocean currents Shortwave radiation Optical raingage SEACAT conductivity and temperature recorders
ADCP	Vertical profile of upper-ocean currents
IMET	Surface wind, relative humidity, barometric pressure Precipitation and temperature of rain Buoy motion (pitch, roll, and heave) Shortwave and longwave incoming radiation Vertical profile of ocean velocity and temperature Seacat recprders
PCM	Vertical profiles of ocean currents, temperature, and conductivity
Acoustic mooring	Surface winds, surface wave field, wave breaking, occurrence of rainfall, entrainment of air, bubble clouds

TABLE 3. Listing of the satellite instruments likely to be available during TOGA COARE during the IOP.

Satellite and sampling frequency	Instruments and resolutions	Geophysical parameters retrieved
GMS (Japan) 1/2–3 hours	**VISSR** Visible—2.5 km Infrared—5 km	Cloud-tracked winds, radiation, convection monitoring precipitation estimates
NOAA (USA NOAA) 4 times per day	**AVHRR** 2 visible & 3 infrared channels—1 km **TOVS (HIRS/MSU)** 1 visible, 19 infared—2.5 km 4 microwave—100 km	Sea surface skin temperature, clouds, radiation, temperature and moisture profiles
DMSP (USA DOD) 4–6 times per day	**OLS** Visible and infrared—1.5 km **SSM/I** 7 microwave–25/15 km **SSM/T(2)** 7 microwave—150 km 5 microwave—15 km	Cloud detection for SSM instruments, Surface wind, speed, integrated water vapor, cloud liquid water, atmospheric temperature and moisture profiles
ERS-1 (ESA) Approximately 1 time per week repeat orbit 3 days	**ATSR** As AVHRR but dual angle—1 km **AMI/SAR** Shared scatterometer/Synthetic aperature radar **ALTIMETER**	Sea surface skin temperature, clouds, radiation, sea surface wind stress, Ocean surface level
TOPEX/Poseidon (USA/France) (NASA/CHES) repeat orbit 10 days	Dual-frequency radar altimeter—20 km Single-frequency radar altimeter—20 km M-wave radiometer	Ocean surface level Integrated water vapor

used in numerical models. Geophysical algorithms that relate the fluxes to observations by spaceborne sensors also need to be adapted to the conditions over the warm pool.

During COARE, air–sea fluxes will be measured by a number of techniques using a wide range of platforms.

(i) *Measurement of air–sea fluxes on ships*

The turbulent fluxes (momentum, sensible, and latent heat) will be measured on ships by eddy correlation, dissipation, and bulk-parameterization methods, and the radiative fluxes by radiometers. The eddy correlation method is the most direct measurement of the turbulent fluxes but it requires careful correction for the motion of the sensors, particularly in the vertical. Dissipation and bulk parameterization are indirect methods and depend on models and assumptions that need to be validated or modified for the unique conditions in the western tropical Pacific.

The advantage of ship measurements is that close attention can be given to the sensors by onboard scientists or technicians and that long time series can be obtained. Due to the slow speed of a ship compared with the temporal variation of the fluxes, a ship is not an optimal platform on which to study spatial variability. Furthermore, flow distortion and heating due to the ship itself need to be taken into account. However, ship flux measurements can be used to study the local forcing and are also valuable for comparison with all other methods.

Presently, three ships, from the United States, Japan, and Australia, have been identified to provide direct turbulent-flux and radiative-flux measurements (panel e, Fig. 14). A schedule of ship intercomparison has been developed so that over the course of the IOP each ship will compare flux measurements while in close proximity with each other. Aircraft–ship intercomparisons are also scheduled.

(ii) *Measurement of air–sea fluxes on aircraft*

Surface turbulent fluxes will be measured by eddy correlation methods using data collected from low-flying aircraft, with the motion of the aircraft corrected

by the navigation system. The advantage of the use of an aircraft over a ship as a flux platform is that the aircraft can measure the spatial variation of the fluxes. Optimal flight patterns have been developed in conjunction with atmospheric boundary-layer studies, and these will be discussed in detail in section 5c.

Surface wind stress will also be derived from microwave scatterometers on aircraft. The geophysical algorithm that links the backscatter observed by the sensor to surface wind vector must be tested in the low-wind and high sea surface temperature conditions during COARE. Scatterometer aircraft will overfly the surface-flux–measuring aircraft and ships in order to maximize the opportunity for calibration whenever possible. Radar measurements of the surface wave field will be made from an aircraft to infer wave influences on surface stress.

(iii) *Measurement of air–sea fluxes on moored buoys*

The TOGA TAO array of moored buoys provides platforms for measurements related to the fluxes. The disadvantage of deriving fluxes from sensors on moored buoys is that the sensors cannot be serviced adequately. A rugged meteorological sensor package (IMET) has been developed and will be located in the center of the IFA. The IMET measures surface horizontal wind speed and direction, relative humidity, air temperature and SST, solar and longwave radiative fluxes, surface pressure, precipitation, and buoy motion. IMET will provide long time series of the air–sea fluxes within the IFA.

(iv) *Estimates of air–sea fluxes from atmospheric and oceanic budgets*

Surface fluxes can be computed as residuals of the balance between the Eulerian storage change and advection. In the atmosphere, the change of storage and advection can be derived from a rawindsonde network. The implementation of a rawinsonde network and its utility in determining the atmospheric energy and water budget are addressed in section 5c. Also, surface fluxes can be computed from ocean-energy and salinity budgets. The ocean observing network that will be used for these budget studies is discussed in section 5e. The measurement of rainfall, an important component of the surface buoyancy forcing of the ocean, is considered in section 5d.

With the difficulties of measuring ocean currents, the fluxes could be derived just from the Lagrangian storage change. The ARGOS-tracked drifters of the TOGA/WOCE Surface Velocity Program (SVP) array will be used to compute the Lagrangian change of heat storage in the mixed layer. With additional installation of salinity sensors, buoyancy flux will also be computed. The drifters also measure surface currents, which, together with surface wind, can be used to understand momentum coupling at the surface.

(v) *Determination of air–sea fluxes from general circulation models*

The ECMWF, the Australian Bureau of Meteorology Research Centre (BMRC), and NOAA/NMC produce surface fluxes from their operational forecast models. Surface and upper-air meteorological reports are objectively assimilated into a first-guess field for the latest forecast. There are plans to assimilate satellite data into these atmospheric models to improve the forecast. Scatterometer winds from ERS-1 will be assimilated into the ECMWF model to produce an improved surface-wind velocity product. Numer-

TABLE 4. List of the research aircraft that will take part in the COARE IOP.

Type	Origin	Schedule	Operations base	Time on station (IFA)	Research hours
Cessna 340	AU/Flinders	Jan 93	KVG	4	100
C-130	UK/MRF	Jan–Feb 93	TSV	5.5	70
L-188	US/NCAR	Nov 92–Feb 93	HIR	3.5	320
WP-3D	US/NOAA	Nov 92–Feb 93	HIR	6	220
WP-3D	US/NOAA	Nov 92–Feb 93	HIR	6	220
DC-8	US/NASA	Jan–Feb 93	TSV	3.5	100
ER-2	US/NASA	Jan–Feb 93	TSV	1	100

ous research studies are under way in data-assimilation and model-based surface-flux computation. Joint efforts between COARE and these operational centers to refocus the numerical studies in the western tropical Pacific have been arranged.

3) Satellite measurements

Spaceborne microwave scatterometers are used to estimate surface wind vectors from which the surface momentum flux can be derived. The active microwave instrument (AMI) on the ERS-1 is scheduled to be in operation during COARE and will measure surface wind vectors at C-band when put in scatterometer mode. However, the sampling may not be adequate to meet all COARE objectives, because the sensor has only half the swath width of the Seasat scatterometer and can only operate in scatterometer mode for part of the time. Furthermore, the observations from the scatterometer may not have the required sensitivity at low winds.

During COARE, surface latent heat flux will be derived from measurements of the operational SSM/I and AVHRR, using bulk-parameterization models. The data will be available from NOAA/NESDIS and NASA Wetnet. Surface solar irradiance will be derived from cloud information provided by sensors on the GMS. These data will be available from ISCCP and NASA Wetnet. The techniques have been demonstrated and validated in the eastern tropical Pacific but have yet to be adapted and evaluated under western tropical Pacific conditions. Supplementary data from operational atmospheric sounders (TOVS and SSMT) will help to derive longwave radiation and sensible heat flux and improve the accuracy and resolution of latent heat-flux retrieval. The methodologies using these data are still in the developmental stages and need to be tested vigorously.

Satellite determination of the surface radiation budget (SRB) is presently the subject of extensive research efforts. There are still a number of scientific questions that need to be addressed before accurate confidence limits can be placed on these satellite estimates. The satellite data (notably GMS visible and IR radiance data) collected during the IOP, together with in situ surface-flux measurements being obtained as part of the SRB pilot study, will serve as a crucial dataset for validating any COARE SRB algorithms. In addition to the long-term SRB validation sites, shortwave radiometers will be part of the meteorological package on the IMET buoy. Shortwave and longwave radiometers will be on a number of COARE ships, and are also located on the islands of Truk, Majuro, and Ponape. There are plans to place another station at Misima. The locations of the stations can be seen in Fig. 14, panel a.

c. The design of the atmospheric component

1) General observational strategy

The strategy for the atmospheric component is to develop an overlapping observational system. With this technique, similar to the type used in GATE and more recently in AMEX (McBride and Holland 1989) and EMEX (Webster and Houze 1991), the consistency of in situ aircraft measurements are checked by the surrounding upper-air network, which provides estimates of gross budgets of moisture, heat, and momentum. Gross budget estimates will be made using well-established budget techniques (e.g., Yanai et al. 1973). Improved assimilation schemes and mesoscale models are expected to contribute significantly to the analysis of COARE observations.

2) Atmospheric convection and the boundary layer

The objectives of TOGA COARE require empirical determination of precipitation, heating, and momentum redistribution throughout the troposphere and the atmospheric boundary layer. It has been proven in previous tropical field programs that the most important observational tools required to document these processes are sounding networks, meteorological radar, and aircraft observations. Consequently, the convective subprogram of TOGA COARE calls for an integrated observational network utilizing these platforms.

(i) *The sounding system*

The sounding network, enhanced with ISS stations, will enable fluxes to be computed as residuals within and about mesoscale convective systems. The COARE sounding network consists of an embellished WWW network in the COARE large-scale domain (panel a, Fig. 14) and the COARE outer sounding array (panel b, Fig. 14), which was described in section 5a. During the IOP, the upper-air stations within the large-scale domain will operate with a frequency of two sondes per day. Within the outer sounding array and the IFA, the frequency of soundings will be four per day.

A major aim of the IOP will be to determine areal estimates of the total flux between the atmosphere and the ocean using residual aerological methods introduced by Yanai et al. (1973). Within the outer sounding array, there will be an average spacing between the sounding sites of about 300–400 km of latitude. In the IFA, the spacing is reduced to about 2°. Thus, within the outer sounding array and the IFA it is probable that useful residual estimates of surface fluxes may be calculated. In the large-scale domain, the greater spacing of the observations and their lower observation frequency cast some doubt that the flux estimates will be useful except when averaged over a much longer period of time. However, all of the data are exceptionally valuable for the definition of atmo-

spheric motion and for providing initial and validation data for models.

Continuous data will be collected, provided by the wind profilers and the RASS of the ISS stations (Fig. 14, panel b), and should prove vital for documenting the horizontal and vertical structure of the boundary layer in the vicinity of deep precipitating systems, including their downdraft wakes. The composite sounding network, along with a 2 day^{-1} frequency of WWW soundings, should provide a continuous record of the background fluxes and boundary-layer structure during the full range of meteorological conditions. The wind profiler and RASS will be the backbone of the sounding-measurement program, with high temporal and spatial resolution in the lower troposphere being of critical importance for monitoring possible rapid changes that might occur during the onset of a westerly wind burst. The ISS array will also enable determination of diurnal variations of the boundary layer.

(ii) *Radar observations*

Panel c of Fig. 14 shows the COARE IOP radar coverage. The two Doppler radars are located on an east–west line, separated by 200 km. Whereas the highest priority of the radar network is to provide estimates of precipitation over the IFA, on occasion the two ships will be moved to within 50 km of each other to perform dual-Doppler experiments. On Manus Island, two Japanese radars (a Doppler radar and a dual linear polarized radar) have been located about 35 km apart.

In their survey or single-Doppler mode, the COARE radars will be able to:

- make quantitative estimates of rainfall amounts over the IFA for most of the IOP,
- partition the rainfall into contributions from convective and stratiform regions of mesoscale convective systems,
- determine the size distributions and other structural characteristics of the mesoscale and convective rainfall-producing entities,
- perform mesoscale analyses of the precipitation patterns that allowed boundary-layer flux and radiation measurements to be stratified into meaningful categories,
- compare rawinsonde residual analyses to actual measurements of precipitation systems in the IFA,
- estimate wind variance of the radial component relative to the radars, and
- measure the vertical profile of divergence in precipitating areas.

In the dual-Doppler mode, the following additional information will be obtained:

- the three-dimensional wind field in mesoscale convective systems,
- the deduction of thermodynamic and water fields from the wind data using a diagnostic "retrieval" technique, and
- a complete analysis of heat, mass, and momentum fluxes and budgets.

(iii) *The aircraft program*

The objectives of TOGA COARE strongly entail empirical determination of precipitation, heating, and momentum redistribution throughout the troposphere and the atmospheric boundary layer, together with radiation distributions and a description of cloud microphysics. It has been proven in previous tropical field programs that the most important observational tools required to document these processes are sounding networks and meteorological radar. However, as shown in recent successful aircraft-based experiments such as EMEX and TAMEX (the Taiwan Atmospheric Meteorological Experiment), airborne measurements of latent and sensible heat fluxes throughout the troposphere and boundary layer have improved dramatically since GATE. In addition, both experiments used airborne Doppler radars.

The airborne platforms are important to the central objectives of COARE for the same reason that the ship array is crucial. That is, they provide coverage of the three-dimensional wind fields and in situ fluxes in the mesoscale convective systems and boundary layer responsible for tropospheric heating and fluxes. The difference is in the type of sampling each provides. The strength of the ship-borne array is its ability to provide a continuous time series in the center of the array throughout the whole project. The limitation of the ships is that they have a view restricted to the fixed vicinity of the ship. The aircraft, being highly mobile, can sense the entirety of a large mesoscale convective system in a few hours. The aircraft can also go to wherever convection is active and obtain intensive sampling in the most relevant parts of the system. By varying the aircraft altitude, the in situ fluxes can be measured in the boundary layer or other important regions of the mesoscale convective complexes.

The meteorological and oceanographic observational systems in the IFA are designed to provide a temporal perspective of phenomena and processes from a fixed location. The aircraft, on the other hand, will provide spatial descriptions of phenomena and processes at specific times. At the same time, the aircraft have the ability to provide vertical distributions of fluxes either from one aircraft in a series of horizontal legs or from multiple aircraft in stacked formation.

EMEX demonstrated the feasibility and effectiveness of probing COARE mesoscale convective sys-

tems with technologically advanced remote sensors (Webster and Houze 1991). Since EMEX, the airborne Doppler systems on the NOAA P3 aircraft have been reconfigured, and an entirely new system (ELDORA), developed by a French–U.S. consortium, will be installed on the NCAR Electra aircraft. These new systems will be able to utilize various forms of two-directional scanning such that the aircraft will be able to measure two components of wind direction at any location in radar range nearly simultaneously. Thus, it will be possible to obtain more truly dual-Doppler coverage in convective systems. Furthermore, the COARE surface-based observation network, within which the aircraft will operate, is far more sophisticated and complete than in previous experiments.

In order to simplify the planning of aircraft missions in a complex and variable meteorological environment, a stratification into five generic synoptic classifications was made in terms of their cloud properties. These are:

Class 0: Minimal cloud or clear conditions representing the undisturbed boundary layer. In Figs. 9a and 9b there are very light wind and clear regions adjacent to the IFA.

Class 1: Cloud areas made up of systems with areas < 6000 km^2 or length scales of order 20–30 km. Figure 9a shows a series of class 1 systems in the vicinity of the IFA stretching zonally as a series of lines. Areas are determined as having an IR temperature < 208 K.

Class 2: Cloud areas made up of elements between 6000 and 20 000 km^2 or length scales of order 100 km. These systems may be seen as discrete and organized entities near the IFA in Fig. 9b.

Class 3: Cloud systems with areas between 20 000 and 60 000 km^2. Length scales of these disturbances span about 250 km. Examples may be seen to the northeast of Australia in Fig. 9a.

Class 4: Very large-scale cloud entities with scales > 60 000 km^2. Figure 9c (iii and iv) shows two examples of this classification. The first (Fig. 9c) appears as part of a very disturbed region along the equator. The second (Fig. 9d) shows two class 4 conglomerations on either side of the equator that have matured into tropical cyclones.

As COARE is basically an interface experiment, aircraft observations will be maximized over the IFA whenever possible where the surface-based observations are concentrated. To allow an orderly selection of missions on a day-by-day basis, a priority system has been developed for the aircraft program that emphasizes the sensing of a full spectrum of weather in the IFA. The priority system attempts to balance flights between boundary-layer missions and convective missions. A considerable effort will be made to sample the rarer classes, 3 and 4, especially when they occur over the IFA or within the outer sounding array.

Although the forms of convection are diverse, an aircraft plan has been developed that encompasses the five cloud categories described above. This has been accomplished by using the aircraft to sample the horizontal structure of the systems for the lower-number classifications and increasing the vertical stacking for higher classification numbers. The generic plans for convection classifications 0–4 are shown in Figs. 15a–e, respectively.

3) The large-scale circulation

A basic aim of COARE is to document the morphology of convective events in the COARE large-scale domain in order to provide a large-scale perspective for the IFA and to produce an observational dataset that will allow the determination of gross interface-flux estimates. To be of utility, the observations must be both frequent and relatively densely spaced. The enhanced sounding system in the large-scale domain, the TOGA profilers located at Christmas Island and Canton Island, the surface wind and temperature network from the TOGA TAO moored buoys, and the WWW network will provide the large-scale surveillance necessary to monitor signals emanating from the COARE region or large-scale influences of the COARE region originating elsewhere.

4) Clouds and radiation

In terms of the general objectives of COARE, the specific study of clouds and radiation in the warm-pool regions of the tropics is germane because of the control clouds have on the surface radiation budget at the surface of the warm pool. Four separate instrument configurations will be used to observe cloudiness and assess the radiation fields in the tropical warm pools:

- **Surface radiometers:** Suites of instruments will be located on oceanographic survey ships, on meteorological ships within the IFA, and at sounding stations with ISS's (panels b and c, Fig. 14.). The instrumentation is basic and measures total downwelling infrared and visible streams at the surface.
- **Airborne radiometers:** Almost all aircraft carry infrared and visible radiometers with the capability of looking upward and downward, which allows the measurement of surface albedo and surface temperature. The two NASA aircraft, the DC-8 and the ER-2, carry much more sophisticated radiation instrumentation. Aircraft have the advantage of allowing the measurement of vertical profiles of radiational heating while in stacked formation.

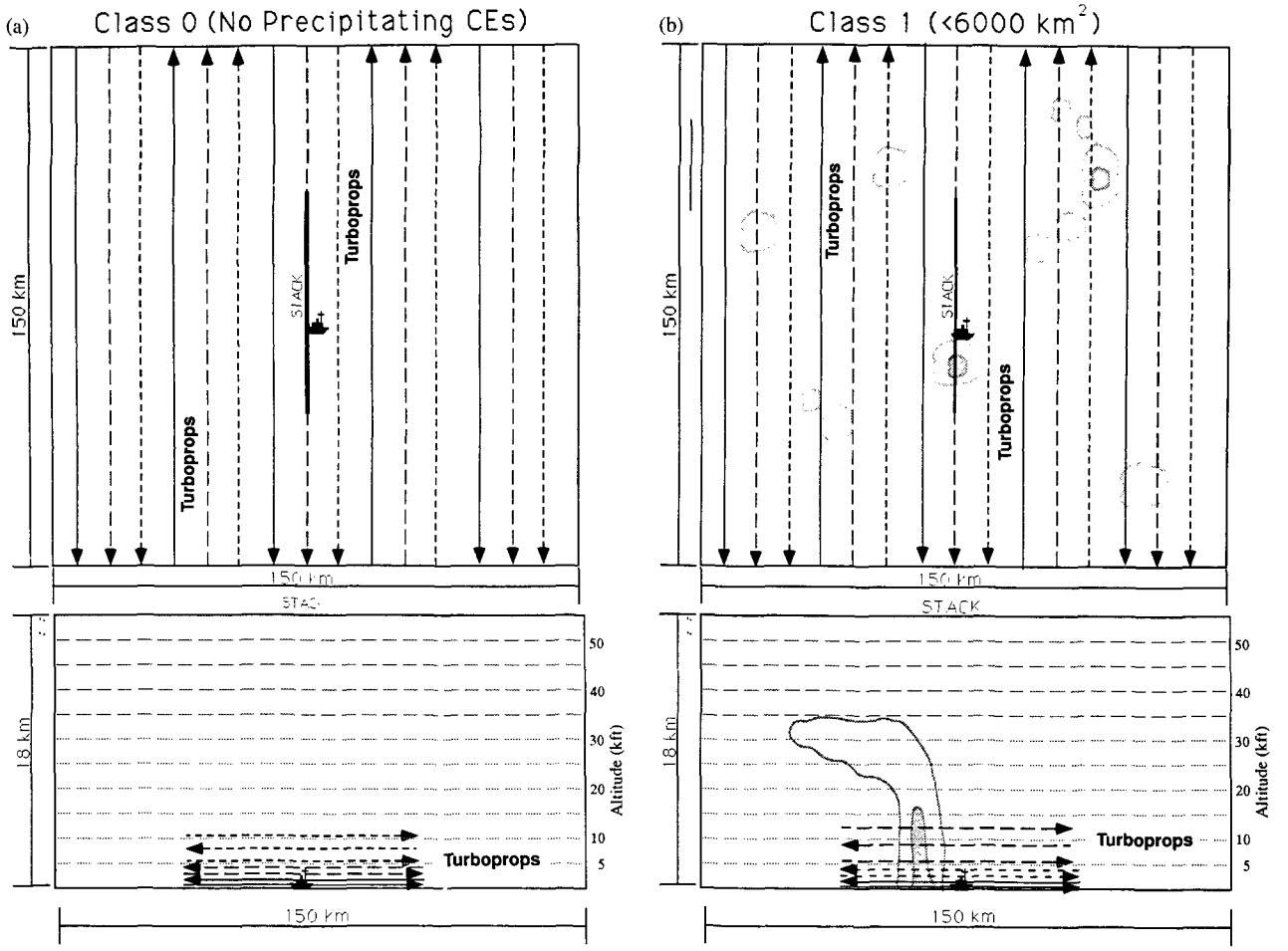

FIG. 15. Generic aircraft plans for the intensive operations phase (IOP) of TOGA COARE, which will be carried out in the intensive flux array (IFA) or within the outer sounding array (OSA). Plans depend on the organization of cloudiness in the region and the location of the convection relative to the IFA. Clouds are classified by the amount of cloud area with an equivalent blackbody temperature < 208 K. Classifications are described in the text and examples are given in Fig. 9. In the figures, the term "turboprops" refers, collectively, to the two NOAA WP-3Ds, the NCAR L-188 Electra, the UK C-130, and the Australian Flinders University Cessna 340. The NASA DC-8 and the ER-2 are identified separately. (a) Flight plans for class O organization. The top half of the diagram shows a plan view of the flight track over a 150 x 150 km domain. The bottom half depicts a vertical cross section (vertical stack) of the flight track that extends through 5 km in the vertical. The small ship symbol denotes the position of one of the ships taking in situ measurements of the fluxes in the IFA. (b) Same as (a) except for class 1 convection. The light and dark hatching denotes radar echo boundaries (10 and 40dBZ) of the convection. The cloud area defined by OLR is generally 25% larger than the radar echoes.

- **Satellite observations:** Cloud extent and height can be determined by regular infrared and visible satellite observations of the GMS and the GOES satellites. These may be supplemented by the polar orbiters. Together, the radiation budget at the top of the atmosphere will be assessed during the entire IOP.
- **The Kavieng PROBE site:** The Kavieng Pilot Radiation Observation Experiment (PROBE) of the Atmospheric Radiation Measurement (ARM) program will maintain a sophisticated array of instruments at Kavieng during the IOP. The instrumentation will include direct measurements of radiative flux with a wide range of instruments and the vertical profiles of wind, temperature, and water vapor from an ISS system. In addition, remote sensing of cloud geometry, particulate size, and other cloud parameters will be made using lidar systems and microwave radiometers. It is planned to overfly the Kavieng site as often as possible, especially with the NASA DC-8.

5) MEASUREMENTS FROM SATELLITE

(i) *Precipitation.* Indirect estimates of rain rate can be made using a time series of visible and infrared images from the GMS satellite. Direct estimates of rain rate can be made using passive microwave data from the SSM/I (e.g., Liu and Curry 1992). In situ observa-

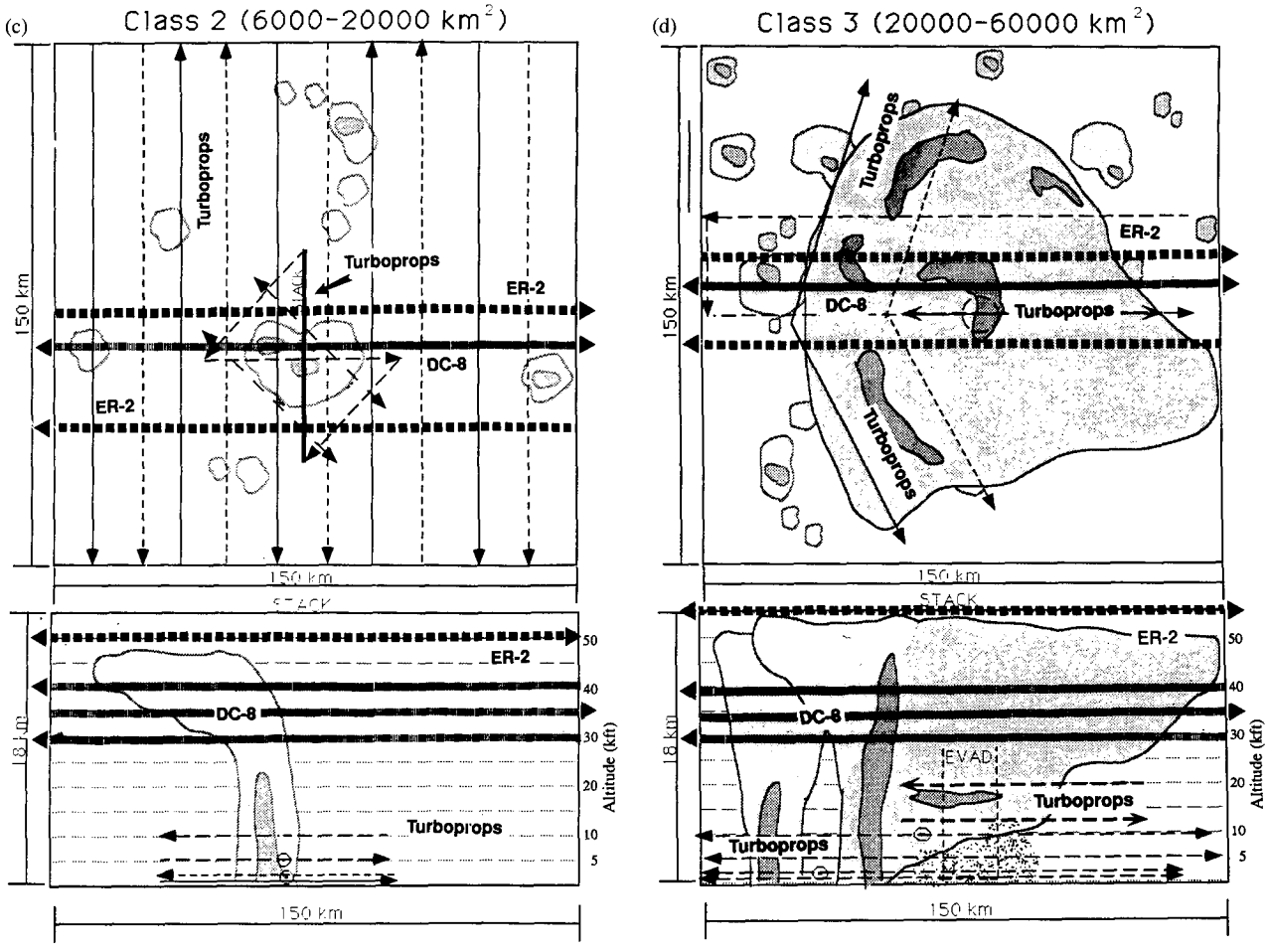

FIG. 15 (continued). Generic aircraft plans for the intensive operations phase of TOGA COARE. (c) Same as (a) except for class 2 convection. In addition to the lower troposphere probing of the turboprops, the ER-2 and the DC-8 would be involved. The domain of the vertical stack is now 15 km deep with the NASA sensing the middle and upper troposphere. In the depiction here, the ER-2 is perfoming a "racetrack" pattern around the disturbance while the DC-8 is making a series of vertical sections through the disturbance. (d) Same as (a) and (c) except for class 3 convection. The domain of the vertical stack is 150 km and 18 km. The circle shows the position of the "EVAD" turboprop pattern, which is a technique for collecting radial velocity information.

tions using radar will provide a unique opportunity to validate existing rain-rate algorithms and provide a test bed for examining hybrid algorithms combining multiple sensors. Surface- and aircraft-based radars will be tuned to the SSM/I algorithms, and all three should be compared and tuned to the PMS drop-size probes on the NOAA P-3. The COARE surface observations also contain a modest pluviograph system so that point checks can be made of satellite-determined precipitation estimates.

(ii) *Atmospheric temperature and moisture profiles.* Atmospheric temperature and moisture profiles are important for determining the atmospheric state, as well as for computing the attenuation of surface variables through the atmosphere. Attention should be focused on microwave instruments (SSM/T and SSM/I) because of their low sensitivity to cloud attenuation. Data from the ISS instruments and enhanced radiosonde network will be used in validating these measurements.

(iii) *Atmospheric radiative fluxes and heating profiles.* Satellite measurements in conjunction with aircraft and surface measurements can be incorporated into analysis schemes that aim at calculating radiative heating profiles. The viability of such an approach was tested in analysis of EMEX data (Webster and Houze 1991). A cloud-radiation experiment has been proposed as a specific element of COARE.

(iv) *Characterization of convective state.* Much of our present knowledge about the organization and propagation of convection over the warm pool has come from time–longitude diagrams of OLR and GMS window-channel brightness temperatures. Active convection is associated with high, cold cloud tops, so

thresholds can be set to distinguish these areas. In addition, for the IOP, the various convective states could be characterized by analyzing spectral and textural features using both GMS and AVHRR data.

d. The design of the oceanographic component

The objectives stated in section 4c cannot be achieved solely from observations—a mix of observations and modeling is planned. The COARE observational strategy is to bridge the time and space scales observed during intensive measurements made in a limited region for 4 months (the IOP) to the large spatial scales of the decade-long TOGA monitoring network, by means of a two-year-long enhanced monitoring (EM) effort in the COARE domain centered in time on the IOP. Model-based analyses of the IOP observations are required to tie the small-scale measurements into the EM array.

1) Observational strategy

The oceanographic component of the COARE field program is a three-dimensional mixed-layer experiment integrated with atmospheric and interfacial components that will provide air–sea fluxes of heat, moisture, and momentum. This mixed-layer experiment is designed to provide enough information to enable accurate modeling of the warm pool, including both the off-equatorial and equatorial regimes. The observations will be capable of resolving the different time and space scales for the diabatic and dynamic responses of the warm pool.

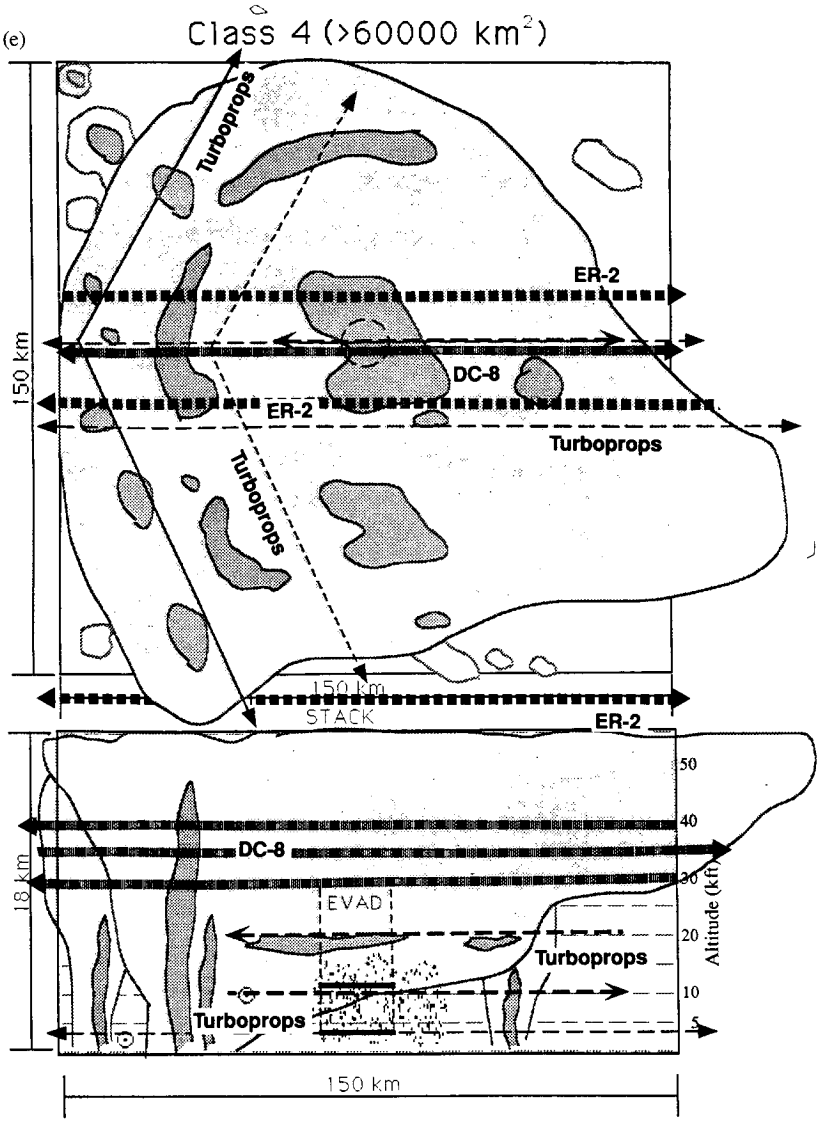

Fig. 15 (continued). Generic aircraft plans for the intensive operations phase of TOGA COARE. (e) Same as (a) and (d) except for class 4 convection. The ER-2 will fly at altitudes in excess of 20 km.

The EM moored oceanographic array will make high temporal resolution measurements at relatively widely spaced locations to obtain statistics that will be used to relate short-term variations to the low-frequency evolution of the warm pool, and to provide a regional context for the oceanographic observations during the IOP. In conjunction with the array of TAO ATLAS moorings and the equatorial current meter moorings supported by the TOGA monitoring, the EM array spans the COARE domain, and concentrates additional observations in the vicinity of 156°E (panel d, Fig. 14). Enhancement of the TOGA drifting buoy and XBT programs will increase the density of observations in the COARE domain.

The IOP measurements will nest additional moored elements within the EM array to obtain time series on even smaller spatial scales, and will include high-resolution mapping of the thermohaline and velocity structure of the upper ocean within and around the array, in order to resolve the many scales of the oceanic response to vigorous atmospheric convection. Lagrangian measurements of surface-layer temperature and salinity will complement the Eulerian observations. The combined moored, shipboard survey, and drifter measurements are meant to provide a

context of horizontal and vertical advective changes in upper-ocean properties within which mixing observations can be interpreted. Vertical velocity estimates cannot be measured in the ocean, but useful estimates will be obtained from the sequential mapping and from horizontal divergences calculated from coherent elements of the IOP array. Shipboard profile measurements of turbulent fluxes will quantify diffusive processes. The locus of the intensive oceanographic measurements during the IOP is within the region of Doppler radar coverage, where air–sea momentum, heat, and moisture fluxes will be provided by the interface and atmospheric components. The composite oceanographic observations during the IOP will also provide an integral constraint on the estimates of net surface fluxes of heat, moisture, and momentum that are obtained by other methods.

2) Observational plan

(i) *Enhanced monitoring*

The enhanced monitoring will provide data to describe the warm-pool response to large-scale meteorological forcing events and, in combination with model data assimilation, the net lateral transport of mass, heat, and salt into the COARE domain. These measurements will provide a context for understanding observations on intermediate scales. In particular, the EM array is designed to detect the equatorial wave response of the tropical ocean to westerly windburst events. This array includes moorings, drifters, and satellite altimetry components as described below.

The TOGA–TAO array consists of ATLAS thermistor-chain moorings along three meridians in the COARE area plus current-meter and additional ATLAS moorings at selected locations along the equator (panel d, Fig. 14) to resolve zonal gradients of temperature and salinity at intermediate scales. Conductivity sensors have been included on a subset of these moorings to measure upper-ocean salinity. An array of current-meter moorings is monitoring the transport fluctuation along the northern coast of Papua New Guinea, which may influence the currents along the equator in the COARE domain.

The maintenance of the large number of ATLAS and current-meter moorings in the EM array is currently shared by French, Japanese, and U.S. research vessels. Special efforts are being made by France to occupy the 156°E line from 10°N to 5°S at 6-month intervals in order to maintain the equatorial current-meter mooring, and to provide an additional hydrographic section for comparison with the ongoing 165°E long time-series section.

Shipboard observations during array deployment and maintenance cruises consist of high-quality upper-ocean CTD (conductivity, temperature, depth) profiles, thermosalinograph time series (providing very high-resolution temperature and salinity data at depths of about 4 m), acoustic Doppler current profiling, and near-surface meteorological observations. CTD profiling is conducted at the mooring sites, and at appropriate locations in between. At mooring sites, several casts are made in order to obtain statistics for calibration of the conductivity sensors.

Upper-ocean, satellite-tracked drifters complement the moored description of upper-ocean currents and thermal structure. The TOGA Pan-Pacific Drifter study will be augmented in the COARE domain by additional drifter releases from research vessels and ships of opportunity. These drifters will also measure salinity variations near 10-m depth. Two types of thermistor-chain drifter will provide high vertical resolution of the thermal structure in the upper 20 or 150 m.

The TOGA ship of opportunity program has three XBT lines that run through the COARE domain (panel a, Fig. 14). During the EM period, additional XBTs will be launched to ensure adequate resolution within the equatorial waveguide. Ships operating on these lines will be equipped with thermosalinographs providing high-resolution temperature and salinity data in the upper 10 m along the ship tracks. The TOGA program plans to launch expendable CTD (XCTD) probes along at least one of these lines in the near future.

The TOPEX/Poseidon and ERS-1 satellites will provide radar altimetric observations, which will be combined with island sea level data and dynamic height calculated from moored temperature and salinity measurements to map sea level fluctuations in the COARE domain. Additional deep-ocean instrumentation on the ATLAS moorings at 2°S, 156°E and 2°S, 165°E (TOPEX/Poseidon crossover points) will provide high-quality time series of dynamic height and sea level for validation studies. The altimeter observations are crucial for providing spatial coverage to completely resolve equatorial wave motions (cf. Delcroix et al. 1991) that connect the COARE domain to the rest of the tropical Pacific Ocean.

AVHRR observations from NOAA polar-orbiting satellites will be collected at ground stations in Guam, Kwajalein, and Townsville, providing full coverage of the COARE domain at 1-km resolution. This high-resolution coverage is necessary to retrieve as much usable sea surface information as possible, and for careful comparison with the numerous in situ measurements of near-surface temperature as well as the shipboard and aircraft-based radiometric measurements of the sea surface. Special attention is being devoted during the IOP to quantifying the "cool-skin" effect, with the objective of improving SST retrieval algorithms.

(ii) *Intensive observations*

The space–time structure of SST and SSS and the processes that determine them are the principal focus of the oceanographic component of the IOP. Studies divide roughly into observations on space scales, which can be called large (zonal and meridional scales of 1000 and 200 km), intermediate (30 to 100 km), and small (less than 30 km). The intermediate scales are chosen to bridge between those of large-scale advection and those upon which fine- and microscale mixing processes operate. The assumption implied is that vertical mixing takes place relatively uniformly over the dominant scales of meteorological forcing (i.e., squalls and disturbances within westerly wind bursts). The importance of the intermediate-scale array is that it will link evolution of large- and small-scale variability to one another so that the overall oceanic observational program will span roughly three orders of magnitude in horizontal scales (i.e., order 0–1000 km).

The moored array for the IOP is defined by a diamond, with its vertices at 2°N and 2°S along 156°E, and on the equator at 154° and 157.5°E (Fig. 3.1.2 draft Ops Plan); these points will have subsurface ADCP (Acoustic Doppler Current Profiler) moorings near ATLAS moorings to provide upper-ocean velocity, temperature, and salinity. Combined with the 156°E equatorial PROTEUS surface current-meter mooring and the two subsurface ADCP moorings, the array provides excellent resolution of the dynamic response of the equatorial waveguide to westerly burst forcing. The array design makes the transition from large-scale measurements to measurements on the smaller scales relevant to mixing studies.

The bulk of the IOP moored array is centered near 2°S, 156°E, collocated with the intensive-flux array in the atmosphere (panel c, Fig. 14). This is necessary to assess the response of the upper ocean to strong buoyancy forcing, including the modulation of turbulent mixing by variations in the relative strengths of mechanical and buoyancy forcing.

The intermediate-scale moored array is sited within the Doppler-radar coverage of the IFA (panel c, Fig. 14). There are two regions of high-quality Doppler radar coverage of about 100 km in diameter. Within one of these regions, moored elements will be deployed with 25-km separation. On these scales, we expect to resolve frontal variability and the response to mesoscale atmospheric disturbances, such as individual members of cloud superclusters. Vertical advection in response to both local forcing and remotely forced equatorial waves will be estimated on these scales. Most of the mixing measurements in COARE will be in the immediate vicinity of the most finely separated moored-array elements.

The more widely spaced four elements will be moored profilers (PCMs) designed to measure currents, temperature, and salinity with 5-m vertical resolution from 20- to 200-m depth. The central element will be an IMET surface mooring carrying an advanced surface meteorological package, current meters, and temperature and salinity recorders. Instruments will be spaced as close as 0.5 m apart in the shallowest 20 m of the water column in order to detect freshwater pools produced by rain events. A moored acoustic device will measure the signatures of rain and wind, as well as bubbles from wave breaking. The distribution of bubbles will be used to infer circulation structures in the near-surface layer.

Shipboard surveys will obtain a sequence of sections of *T, S,* and horizontal velocity over the upper ocean during the IOP, from which nearly synoptic maps can be constructed. These will provide resolution of *T, S,* and velocity on scales smaller than the minimum moored-array element separation of 25 km, over distances intermediate to the IOP array and the EM array, and will thus provide information about the horizontal gradients of these properties on a variety of scales.

The research vessel (R/V) Wecoma will cover horizontal scales of 1–100 km by steaming in a butterfly pattern around Moana Wave (panel e, Fig. 14) as rapidly as possible, measuring temperature, salinity, and horizontal velocity in the upper ocean, and meteorological fluxes in the lower boundary layer of the atmosphere. At the beginning and end of each cruise, the sampling pattern will be doubled in size to gain additional gradient information. The oceanographic sampling will include the upper 200 m by using a 150-kHz Doppler acoustic profiler to measure velocity and towed Sea Soar to map three-dimensional structures in temperature and salinity.

The R/V Franklin will cover horizontal scales comparable to the 100-km dimension of the intermediate moored array, but in a Lagrangian framework centered on an upper-ocean drifting buoy. Plans are to deploy the buoy so it will move through the IFA, recovering and redeploying the buoy when it moves out of the region of precipitation coverage.

R/V Le Noroit will provide important information on meridional scales up to 1000 km by making Seasoar, ADCP, and other measurements in a meridional section along 156°E to fill in between the moored elements. An experimental microwave radiometer (ESTAR) will be deployed on Noroit in order to determine its effectiveness in measuring the SSS and SST fields.

The quantification (and ultimately, parameterization) of vertical mixing is receiving special emphasis in COARE. Turbulence measurements will be made off the equator with the objective of observing changes in

mixing between light wind conditions and westerly bursts in an area reasonably representative of the bulk of the warm pool, and additional measurements will be made on the equator where the mean vertical shear is high, and where changes of the vertical shear associated with the Yoshida jet response to a westerly burst will be highest.

To obtain an effective time series of vertical mixing, the Moana Wave will profile at relatively high frequency within a few miles of the IMET mooring for a large portion of the IOP. Free-fall (rise) profilers will measure pressure, temperature, conductivity, temperature microstructure, and velocity microstructure. During shorter portions of the IOP, Hakuho Maru and Natsushima will support turbulence measurements on the equator, and Franklin will make towed turbulence measurements in a Lagrangian framework within the IFA.

The microstructure data will be used to estimate the buoyancy frequency, vertical scales of turbulent overturns, the diffusive dissipation rate for temperature fluctuations, and the viscous dissipation rate for turbulent kinetic energy. Depending on winds and currents, four to six profiles an hour should be obtained. To measure vertical shear, Moana Wave will also profile continuously with a 161-kHz high-resolution Doppler sonar system using coded pulses to obtain a tenfold reduction in noise variance compared to a conventional Doppler profiler. It should obtain good data to at least 300 m. The motions associated with the internal wave field will be resolved by this sonar, allowing the separation of internal and external sources for changes in turbulent kinetic energy.

Station-keeping vessels supporting the interface and atmospheric components will also make certain standard oceanographic observations. These include CTD profiles four or more times per day to at least 500 m and continuous acoustic Doppler current-profile measurements of the upper 300 m.

The Doppler radar vessel R/V John V. Vickers will support special optical observations aimed at quantifying the penetrating radiation and the divergence of the radiative fluxes across the spectrum. Chlorophyll and productivity measurements will determine the biological contributions to variability of the radiant heating in the upper ocean. Horizontally scanning acoustic Doppler current measurements will characterize and quantify the coherent structures in the near-surface velocity field on scales of 2 to 400 m.

Plans include special aircraft-based radiometric measurements of SST during the IOP. These observations will provide nearly synoptic small-scale context for the detailed in situ upper-ocean measurements.

Drifting-buoy deployments are planned during the IOP in order to keep the population of drifters sufficiently dense within the COARE domain. The timing and location of launch will depend somewhat on the (unpredictable) dispersion of drifters during the actual experiment.

3) Calibration and intercomparison

Special attention has been directed toward issues of instrumental calibration and intercomparison, in order to achieve the highest accuracies and precision possible, and to identify and understand the inevitable discrepancies that appear in overlapping observations. During the design of the oceanographic observing system for the IOP, attention was given to having the Seasoar-towed CTD measurements made near PCMs in order to augment the calibration of the moored measurements, and also to provide a touchstone for all Seasoar systems. Some special intercomparison efforts have been scheduled; for example, the Hakuho Maru and Moana Wave will make one-day-long, side-by-side comparisons of their microstructure measurements. Salinity calibration procedures have been developed to provide maximum consistency between the various observations.

6. Summary

The ultimate aim of the TOGA program is to develop a forecasting system for the variability of the coupled ocean–atmosphere system on the time scales ranging from months to years. In this document we have described one component of that effort. TOGA COARE is an observational and modeling program aimed at understanding the basic processes that maintain the warmest waters of the oceans and the role these warm pools play in determining the mean state and variability of climate.

The design of an experiment to study the structure of the warm pools is very complicated and is predicated on the sensing of phenomena that span wide space and time scales and exist within both the ocean and the atmosphere. To accomplish this task, three components were designed: interface, atmosphere, and ocean. With the basic task of obtaining a dataset that will allow the study of the local and remote modes of communication between the atmosphere and the ocean, a composite oceanography–meteorology experiment was developed.

Between November 1992 and February 1993, the international scientific community will pool its resources in the western Pacific Ocean for the field phase of TOGA COARE. In this document, we have concentrated on the field phase of COARE. However, the IOP and the enhanced monitoring effort constitute only the

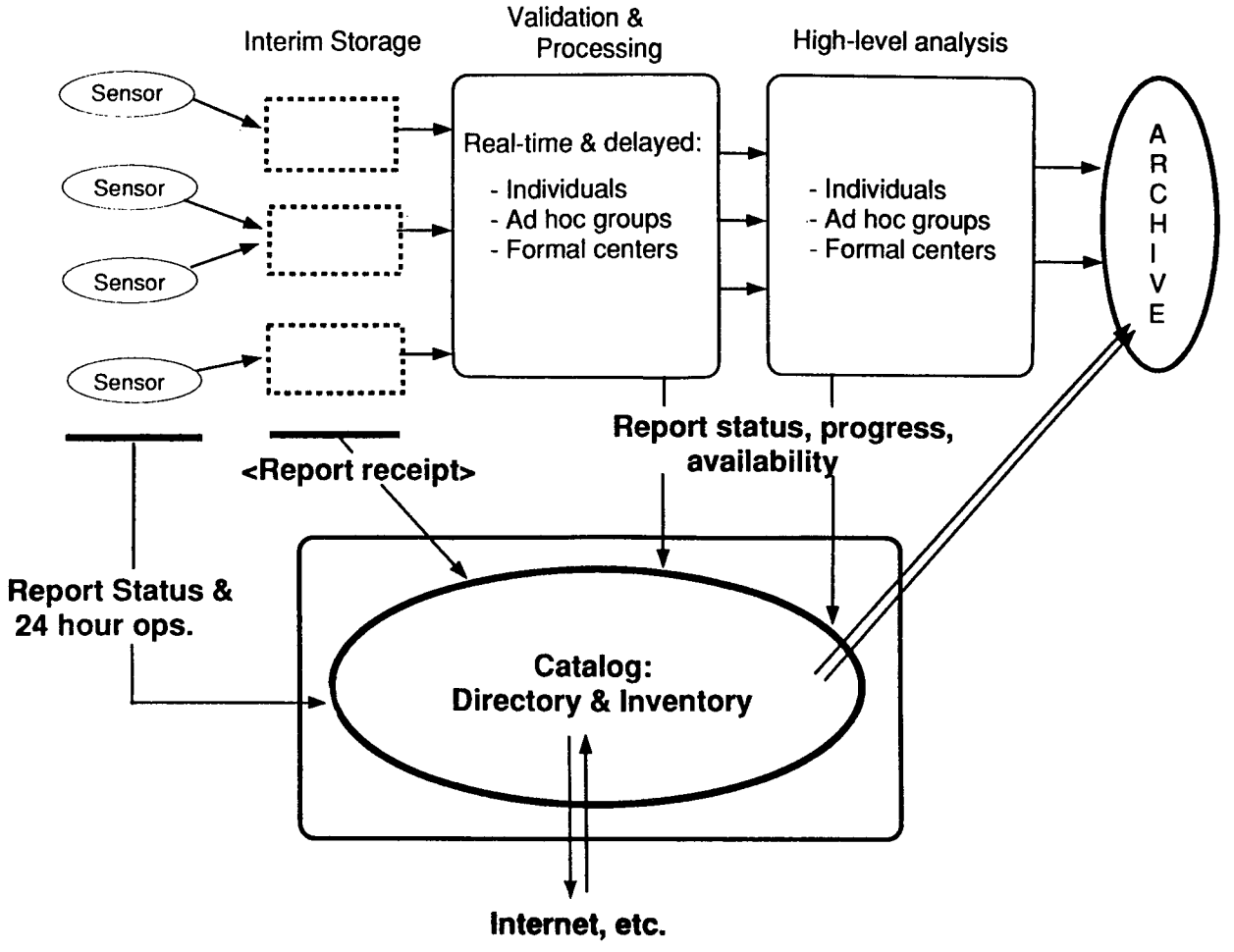

FIG. 16. Schematic diagram portraying the flow of data from the sensor in the field to the accessing of the validated and processed data by the user. Data will be kept in interim storage until it is validated and processed by the appropriate investigator or laboratory. Validated data are placed in a permanent archive. The passage of data between measurement and archiving is monitored by a catalog that acts as a data directory and inventory. Access to the catalog will be through INTERNET, which will detail the form, location, and accessibility of all of the COARE data.

beginning of the research effort. Diagnosis of the data is meant to lead toward better algorithms for remotely sensed data for the eventual use as initialization data for operational climate prediction models. At the same time, the processes uncovered in COARE should lead to better models, especially in the warm-pool regions of the tropical oceans.

TOGA COARE has made a commitment to communicate appropriate data in real time to the international operational meteorological and oceanographic centers. For example, surface data and atmospheric-sounding data will be placed on the GTS for dissemination immediately after the data are collected to be used in routine atmospheric forecast models and experimental ocean prediction models. Thus, the data obtained will also have an immediate utility to the community.

In the years to come, the success of TOGA COARE will be judged by the number of investigators who will use the data collected during the field phase. As the data will be used for a large variety of purposes, including diagnostic studies, model initialization and validation, and algorithm development, it is necessary to set up a system that will allow the community rapid accessibility to the data. Figure 16 shows a schematic of the data flow, cataloguing, and archiving. The upper path shows the route of data between the sensor and its final archiving. As the data are taken, they are accepted into an interim archive. The data is validated and processed by an assortment of groups ranging from individual principal investigators who may have collected the data, to formal research centers. The data are then subjected to high-level analysis before being finally archived. In all of the stages between

measurement and archiving, the progress of the data is stored in a data catalog. It is planned that the scientific community at large may access the catalog through Internet in order to assess the status of the processing of the data, its location, and the mode of accessing the product.

Acknowledgments. We would like to dedicate this paper to the memory of Stanley P. Hayes whose contribution to TOGA and TOGA COARE, both in science and in spirit, are beyond measurement.

The scientific definition and design of TOGA COARE has evolved through the distillation of ideas and concepts from a large group of scientists over a number of years. Science working groups in the participating nations have taken the concept of COARE and have rendered a balanced scientific program and produced a viable experimental design. The International TOGA Panel has acted as the scientific oversight of COARE and has helped foster an international effort of eighteen nations: Australia, the Federated States of Micronesia, France, Germany, Indonesia, Japan, Nauru, New Zealand, Papua New Guinea, People's Republic of China, Philippines, Russia, Singapore, the Solomon Islands, South Korea, Taiwan, the United Kingdon, and the United States, all of which will participate in the field phase. These scientific and operational contributions and the international spirit they have engendered form the backbone of TOGA COARE.

The organization of TOGA COARE has presented a number of unique challenges. Being, by definition, an interdisciplinary effort, scientists have had to adapt to different modes of operation and emphases, and funding sources have been spread across a number of agencies. In the United States, an Interagency Group (IAG) made up of representatives from NOAA, NASA, NSF, and ONR was formed to tackle the multiagency funding questions. The ability of TOGA COARE to enter its field phase is a result of the success of the pioneering endeavor of the IAG.

The implementation of TOGA COARE would not have been possible without the dedicated effort and leadership of Dr. D. Carlson, the director of TOGA COARE International Project Office (TCIPO), and his staff. We are also indebted to Dr. J. Kuettner, who acted as the interim director of the TCIPO and who once again provided great mentorship for an experimental program, and to Dr. E. Lindstrom, the former assistant director of TCIPO. The support of the International TOGA Project Office in Geneva is gratefully acknowledged, especially with the help provided in the upgrading of the WMO aerological sounding network in the COARE domain. Thanks are also due to the scientists who developed the aircraft, radar, and oceanographic sounding implementation plans and who provided cohesion between disparate modes of operation by identifying common scientific goals and developing observational techniques to explore them.

We would like to thank Brigitte Baeuerle of the TCIPO for her technical help in producing Fig. 14 and to J. Curry for comments on the manuscript. R. Houze, Jr., and S. Chen provided Fig. 9 and F. Marks is largely responsible for Fig. 15.

This work was supported jointly by the NSF Division of Oceanography through Grants OCE-8916051 and OCE-9024434, and the NSF Division of Atmospheric Sciences through Grants ATM-8910536 and ATM-9024434.

References

Bean, B.R., and R.F. Reinking, 1978: Marine turbulent boundary layers fluxes of water vapor, sensible heat, and momentum during GATE. *Turbulent Fluxes through the Sea Surface, Wave Dynamics, and Prediction,* A. Favre and K. Hasslemann, Eds., Plenum Press, 21–33.

Betts, A.K., and W. Ridgeway, 1988: Coupling of the radiative, convective, and surface fluxes over the equatorial Pacific. *J. Atmos. Sci,* **45,** 522–536.

Blanc, T.V., 1985: Variation of bulk-derived surface flux stability, and roughness results due to the use of different transfer coefficient schemes. *J. Phys. Oceanogr.,* **5,** 650–669.

Brainerd, K., and M. Gregg, 1991: Preliminary results of the COARE microstructure pilot. *TOGA Notes,* **4,** 1–6.

Cane, M.A., 1980: On the dynamics of equatorial currents, with application to the Indian Ocean. *Deep-Sea Res.,* **27,** 525–544.

——, 1990: Forecasting El Niño with a geophysical model. *Teleconnections Linking Worldwide Climate Anomalies,* M.H. Glantz, R.W. Katz, and N. Nicholls, Eds., Cambridge University Press, 345–370.

——, and S.E. Zebiak, 1985: A theory for El Niño and the Southern Oscillation. *Science,* **228,** 1084–1087.

Chen, D., and L.M. Rothstein, 1991: Modeling the surface mixed layer structure in the western equatorial Pacific. *TOGA Notes,* **2,** 13–16.

Chu, P.C., and R.W. Garwood, 1990: On the two-phase thermodynamics of the coupled cloud-ocean mixed layer. *J. Geophys. Res.,* **96** (suppl.), 3425–3436.

Cornejo-Garrido, A.G., and P.H. Stone, 1977: On the heat balance of the Walker Circulation. *J. Atmos. Sci.,* **34,** 1155–1162.

Delcroix, T., J. Picaut, and G. Eldin, 1991: Equatorial Kelvin and Rossby waves evidenced in the Pacific Ocean through Geosat sea level and surface current anomalies. *J. Geophys. Res.,* **96** (suppl.), 3249–3262.

——, G. Eldin, M.-H. Radenac, J. Toole, and E. Firing, 1992: Variation of the western equatorial Pacific Ocean, 1986–1988. *J. Geophys. Res.,* **97,** 5423–5446.

Eriksen, C.C., M.B. Blementhal, S.P. Hayes, and P. Ripa, 1983: Wind-generated equatorial waves observed across the Pacific Ocean. *J. Phys. Oceanogr.,* **13,** 1622–1640.

Esbensen, S.K., and Y. Kushnir, 1981: The heat budget of the global ocean: An atlas based on estimates from surface marine observations. Climate Research Inst. Rep. No. 29. Oregon State University, 27 pp.

Gautier, C., 1978: Some evidence of cool surface water pools associated with mesoscale downdrafts during GATE. *J. Phys. Oceanogr.,* **8,** 162–166.

Gent, P.R., 1991: The heat budget of the TOGA-COARE domain in an ocean model. *J. Geophys. Res.,* **96,** suppl, 3323-3330.

Geisler, J.E., M.L. Blackmon, G.T. Bates, and S. Munoz, 1985: Sensitivity of January climate response to the magnitude and position of equatorial Pacific sea surface temperature anomalies. *J. Atmos. Sci.,* **42,** 1037–1049.

Godfrey, J.S., and E. Lindstrom, 1988: On the heat budget of the equatorial west Pacific surface mixed layer. *J. Geophys. Res.,* **94,** 8007–8017.

——, M. Nunez, E.F. Bradley, P.A. Coppin, and E.J. Lindstrom, 1991: On the net surface heat flux into the western equatorial Pacific. *J. Geophys. Res.,* **96** (suppl.), 3391–3400.

Gordon, C., and R. A. Corry, 1991: A model simulation of the seasonal cycle in the tropical Pacific Ocean using climatological and modelled forcing. *J. Geophys. Res.,* **96,** 847–868.

Graham, N.E., and W.B. White, 1988: The El Niño cycle: A natural oscillator of the Pacific ocean-atmosphere system. *Science,* **240,** 1293–1302.

Greenhut, G.K., 1978: Correlations between rainfall and sea surface temperature during GATE. *J. Phys. Oceanogr.,* **8,** 1135–1138.

Gregg, M.C., H. Peters, J.C. Wesson, N.S. Oakey, and T.J. Shay, 1985: Intensive measurements of turbulence and shear in the equatorial undercurrent. *Nature,* **318,** 140–144.

Gutzler, D.S., and D.E. Harrison, 1987: The structure and evolution of seasonal wind anomalies over the near-equatorial eastern Indian and western Pacific oceans. *Mon. Wea. Rev.*, **115,** 169–192.

Harrison, D.E., and P.S. Schopf, 1984: Kelvin wave–induced anomalous advection and the onset of surface warming in El Niño events. *Mon. Wea. Rev., 112,* 923–933.

——, and B.S. Giese, 1988: Remote westerly wind forcing of the eastern equatorial Pacific: Some model results. *Geophys. Res. Lett.,* **8,** 804–807.

Hartmann, D., H. Hendon, and R.A. Houze, 1984: Some implications of the mesoscale circulations in tropical cloud clusters for large-scale dynamics and climate. *J. Atmos. Sci.,* **41,** 113–121.

Hirst, A.C., 1988: Slow instabilities in tropical ocean basin–global atmospheric models. *J. Atmos. Sci.,* **45,** 850–852.

Hoskins, B.M., H.H. Hsu, I.N. James, M. Masutani, P.D. Sardeshmukh, and G.H. White, 1989: Diagnostics of the Global Atmospheric Circulation Based on ECMWF Analyses, 1979-1989. WCRP-27, WMO/TD-No. 326, World Meteorological Organization, 217 pp.

Hsiung, J., 1985: Estimates of global oceanic meridional heat transport. *J. Phys. Oceanogr.,* **11,** 1405–1413.

Keen, R. A., 1982: The role of cross-equatorial tropical cyclone pairs in the Southern Oscillation. *Mon. Wea. Rev.,* **110,** 1405–1416.

——, 1988: Equatorial westerlies and the Southern Oscillation. Proc. U.S. TOGA Western Pacific Air-Sea Interaction Workshop, Honolulu, R. Lukas and P. Webster, Eds., U.S. TOGA Rept. USTOGA-8, University Corporation of Atmospheric Research, 121–140.

Keenan, T., and R.E. Carbone, 1992: A preliminary morphology of convective storms in tropical northern Australia. *Quart. J. Roy. Meteor. Soc.* (in press).

Knox, R., and D. Halpern, 1982: Long range Kelvin wave propagation of transport variations in Pacific Ocean equatorial currents. *J. Mar. Res.,* **40,** 329–339.

Large, W.G., and S. Pond, 1982: Sensible and latent heat flux measurements over the ocean. *J. Phys. Oceangr.,* **12,** 464–482.

Lau, K.-M., and P.H. Chan, 1986: The 40–50 day oscillation and ENSO: A new perspective. *Bull. Amer. Meteor. Soc.,* **67,** 533–534.

——, and ——, 1988: Intraseasonal and interannual variations of tropical convection: A possible link between the 40-day mode and ENSO. *J. Atmos. Sci.,* **45,** 950–972.

——, L. Peng, C.H. Sui, and T. Nakazawa, 1988: Dynamics of super cloud clusters, westerly wind burst, 30–60 day oscillations and ENSO: A unified view. *J. Meteor. Soc. Japan,* **67,** 205–219.

Lindstrom, E.J., R. Lukas, R. Fine, E. Firing, S. Godfrey, G. Meyers, and M. Tsuchiya, 1987: The Western Equatorial Pacific Ocean Circulation Study. *Nature,* **330,** 533–537.

Lindzen, R.D., 1967: Internal equatorial waves in shear flow. *J. Atmos. Sci.,* **27,** 394–407.

Liu, G., and J.A. Curry, 1992: Retrieval of precipitation from satellite microwave measurements using both emission and scattering. *J. Geophys. Res.,* in press.

Liu, W.T., K.B. Katsaros, and J.A. Businger, 1979: Bulk parameterization of air-sea exchange in heat and water vapor including molecular constraints at the interface. *J. Atmos. Sci.,* **36,** 1722–1735.

Lukas, R., 1988: On the role of western Pacific air–sea interaction in the El Niño/Southern Oscillation phenomenon. *Proc. of the U.S. TOGA Western Pacific Air–Sea Interaction Workshop,* Honolulu, 16–18 September, 1987. R. Lukas and P. Webster, Eds., U.S. TOGA Rept. USTOGA-8, Univ. Corp. Atmos. Res., 43–69.

——, 1989: Observations of air–sea interactions in the western Pacific warm pool during WEPOCS. Proc. Western Pacific Int'l. Meeting and Workshop on TOGA COARE, Institut Francais de Recherche Scientific pour le Développement en Coopération (ORSTOM), Noumea, New Caledonia.

——, 1990a: Freshwater input to the western equatorial Pacific Ocean and air-sea interaction. *Air–Sea Interaction in Tropical Western Pacific, Proc. US-PRC Int'l. TOGA Symp.,* Beijing, China, Ocean Press, 305–327.

——, 1990b: The role of salinity in the dynamics and thermodynamics of the western Pacific warm pool. *Int'l. TOGA Scientific Conf. Proc.,* WCRP-43, WMO/TD No. 379, 73–81.

——, 1991: The diurnal cycle of sea surface temperatures in the western equatorial Pacific. *TOGA Notes,* **2,** 1–5.

——, and E. Lindstrom, 1991: The mixed layer of the western equatorial Pacific Ocean. *J. Geophys. Res.,* **96,** suppl., 3343–3357.

——, S.P. Hayes, and K. Wyrtki, 1984: Equatorial sea level response during the 1982-83 El Niño. *J. Geophys. Res.,* **89,** 10 425–10 430.

Luther, D.S., D.E. Harrison, and R.A. Knox, 1983: Zonal winds in the central equatorial Pacific and El Niño. *Science,* **222,** 327–330.

Machado, L.A.T., N. DesBois, and J.-Ph. Duval, 1992: Structure and characteristics of deep convective systems over tropical Africa and the Atlantic Ocean, *Mon. Wea. Rev.,* **120,** 392–406.

——, and W.B. Rossow, 1992: Structure, characteristics, and radiative properties of tropical cloud clusters. *Mon. Wea. Rev.,* submitted.

Madden, R., and P. Julian, 1972: Detection of a 40–50-day oscillation in the tropical Pacific. *J. Atmos. Sci.,* **28,** 702–708.

McBride, J., and G. Holland, 1989: The Australian Monsoon Experiment (AMEX): Early Results, *Aust. Met. Mag.,* **37,** 23–35.

McCreary, J.P., Jr., and D.L.T. Anderson, 1991: An overview of coupled ocean-atmosphere models of El Niño and the Southern Oscillation. *J. Geophys. Res.,* **96** (suppl.), 3125–3150.

McPhaden, M.J., and S.P. Hayes, 1991: On the variability of winds, sea surface temperature and surface layer heat content in the western equatorial Pacific. *J. Geophys. Res.,* **96** (suppl.), 3331–3342.

——, H.P. Freitag, S.P. Hayes, B.A. Taft, Z. Chen, and K. Wyrtki, 1988: The response of the equatorial Pacific Ocean to a westerly wind burst in May 1986. *J. Geophys. Res.,* **93,** 10 589–10 603.

——, S.P. Hayes, L.J. Mangum, and J.M. Toole, 1990: Variability in the western equatorial Pacific Ocean during the 1986–87 El Niño/Southern Oscillation event. *J. Phys. Oceanogr.,* **20,** 190–208.

Meehl, G.A., 1987: The annual cycle and interannual variability in the tropical Pacific and Indian ocean regions. *Mon. Wea. Rev.,* **115,** 27–50.

——, and W.M. Washington, 1986: Tropical response to increase CO_2 in a GCM with a simple mixed layer ocean: Similarities to an observed Pacific warm event. *Mon. Wea. Rev.,* **114,** 667–674.

Meyers, G., and J.-R. Donguy, 1984: The North Equatorial Countercurrent and heat storage in the western Pacific Ocean during 1982-83. *Nature,* **312,** 258–260.

——, J.-R. Donguy, and R.K. Reed, 1986: Evaporative cooling of the western equatorial Pacific Ocean by anomalous winds. *Nature,* **323,** 523–526.

Miller, J., 1976: The salinity effect in a mixed layer ocean model. *J. Phys. Oceanogr.,* **6,** 29–35.

Miller, M.J., A.C.M. Beljaers, and T.N. Palmer, 1992: The sensitivity of the ECMWF model to the parameterization of evaporation from the tropical oceans. *J. Climate,* **5,** 418–434.

Molinari, R.L., and D.V. Hansen, 1987: Observational studies of near-surface thermal budgets in the tropics: Review, evaluations, and recommendations. *Further Progress in Equatorial Oceanography,* E.J. Katz and J.M. Witte, Eds., Nova University Press, 421–438.

Moore, D.W., and S.G.H. Philander, 1977: Modeling of the tropical

oceanic circulation. *The Sea,* vol. 6, E.D. Goldberg et al., Eds., Wiley (Interscience), 319–361.

Moum, J.N., D.R. Caldwell, and C.A. Paulsen, 1989: Mixing in the equatorial surface layer and thermocline. *J. Geophys. Res.,* **94,** 2005–2021.

Moura, A.D., and J. Shukla, 1983: On the dynamics and simulation of tropical cumulonimbus and squall lines. *Quart. J. Roy. Meteor. Soc.,* **102,** 373–394.

Nakazawa, T., 1988: Tropical super-clusters under intraseasonal variation. *Japan–U.S. Workshop on the ENSO Phenomena,* University of Tokyo, Meteorology Rep. #88-1, Department of Meteorology, Geophysical Institute, 76–78.

National Academy of Sciences, 1986: *U.S. Participation in the TOGA Program, a Research Strategy.* National Academy Press, 72 pp.

National Research Council (NCR), 1990: *TOGA: A review of progress and future opportunities.* National Academy Press, 66 pp.

Niiler, P., and J. Stevenson, 1982: The heat budget of tropical ocean warm-water pools. *J. Mar. Res.,* **40,** 465–480.

Ostapoff, F., and S. Worthem, 1974: The intradiurnal temperature variation in the upper ocean layer. *J. Phys. Oceanogr.,* **4,** 601–612.

——, Y. Tarbeyez, and S. Worthem, 1973: Heat flux and precipitation estimates from oceanographic observations. *Science,* **180,** 960–962.

Palmer, T.N., and D.A. Mansfield, 1984: Response of two atmospheric general circulation models to sea-surface temperature anomalies in the tropical east and west Pacific. *Nature,* **310,** 483–485.

Philander, S.G.H., 1990: *El Niño, La Niña, and the Southern Oscillation.* R. Dmowska and J.R. Holton, Eds., Academic Press, 293 pp.

Price, J.F., R.A. Weller, and R. Pinkle, 1986: Diurnal cycling: Observations and models of the upper ocean response to diurnal heating, cooling, and wind mixing. *J. Geophys. Res.,* **91,** 8411–8427.

Ramanathan, V., 1987: Atmospheric general circulation and its low frequency variance: Radiative influences. *J. Meteor. Soc. Japan,* **65,** 151–175.

——, and W. Collins, 1991: Thermodynamic regulation of ocean warming by cirrus clouds deduced from observations of the 1987 El Niño. *Nature,* **351,** 27–32.

Rasmusson, E., and T.H. Carpenter, 1983: The relationship between the eastern equatorial Pacific sea surface temperatures and rainfall over India and Sri Lanka. *Mon. Wea. Rev.,* **111,** 354–384.

Reed, R.J., and E.E. Recker, 1971: Structure and properties of synoptic-scale wave disturbances in the equatorial western Pacific. *J. Atmos. Sci.,* **28,** 1117–1133.

Reed, R.K., 1985: An estimate of the climatological heat fluxes over the tropical Pacific Ocean. *J. Climate Appl. Meteor.,* **24,** 833–840.

Sadler, J., M.A. Lander, A.M. Hori, and L.K. Oda, 1987: Tropical marine climatic atlas, Volume II, Pacific Ocean. UHMET87-02, Department of Meteorology, University of Hawaii, 27 pp.

Sarachik, E.S., 1978: Tropical sea surface temperature: An interactive one-dimension atmosphere–ocean model. *Dyn. Atmos. Oceans,* **2,** 455–469.

Seager, R., S.E. Zebiak, and M.A. Cane, 1988: A model of the tropical Pacific sea surface temperature climatology. *J. Geophys. Res.,* **93,** 1265–1280.

Seguin, W.R., and K.B. Kidwell, 1980: Influence of synoptic-scale disturbances on surface fluxes of latent and sensible heat. *Deep-Sea Res.,* **26,** 51–64.

Shukla, J., and D.A. Paolina, 1983: The Southern Oscillation and long range forecasting of the summer monsoon rainfall over India. *Mon. Wea. Rev.,* **111,** 1830–1837.

Taylor, R., 1973: An atlas of Pacific rainfall. Rep. HIG-73-9, Hawaiian Inst. of Geophys., Honolulu, Univ. Hawaii, 7pp, 13 figures.

Thompson, R.M., Jr., S.W. Payne, E.E. Recker, and R.J. Reed, 1979: Structure of synoptic-scale wave disturbances in the intertropical convergence zone of the eastern Atlantic Ocean. *J. Atmos. Sci.,* **36,** 53–71.

Weare, B.C., P.T. Strub, and M.D. Samuel, 1981: Annual mean surface heat fluxes in the tropical Pacific Ocean. *Mon. Wea. Rev.,* **115,** 2687–2698.

Webster, P.J., 1983: The large scale structure of the tropical atmosphere. *General Circulation of the Atmosphere,* Eds. B. M. Hoskins and R. Pearce, Academic Press, 235–275.

——, 1991: Ocean–atmosphere interaction in the tropics. ECMWF Seminar Series: Interaction of the Mid-Latitudes and the Tropics, European Centre of Medium-Range Weather Forecasting, Reading, U.K., 67–116.

——, and H-. R. Chang, 1991: An Atlas of Near-equatorial Winds; 1986–1989. Department of Meteorology, Pennsylvania State University Technical Note, 486 pp.

——, and R.A. Houze, Jr., 1991: The Equatorial Mesoscale Experiment (EMEX): An overview. *Bull. Amer. Meteor. Soc.,* **72,** 1481–1505.

World Climate Research Programme (WCRP), 1985: Scientific plan for the Tropical Ocean Global Atmosphere Programme. WCRP publication #3, World Meteorological Organization, Geneva, 146 pp.

——, 1986: International implementation plan for TOGA. ITPO document #2 (second edition), World Meteorological Organization, Geneva, 96 pp.

Wyrtki, K., 1965: The average annual heat balance of the North Pacific Ocean and its relation to ocean circulation. *J. Geophys. Res.,* **70,** 4547–4559.

——, and G. Meyers, 1976: The trade wind field over the Pacific Ocean. *J. Appl. Meteor.,* **15,** 698–704.

Yanai, M., S. Esbensen, and J.H. Chu., 1973: Determination of the bulk properties of tropical cloud clusters from large-scale heat and moisture budgets. *J. Atmos. Sci.,* **30,** 11–27.

Young, G.S., D.V. Ledvina, and C.W. Fairall, 1991: Influence of precipitating convection on the surface energy budget observed during a TOGA pilot cruise in the tropical western Pacific Ocean. *J. Geophys. Res.,* in press.